Submitted to the European Physical Journal C

ANL-HEP-PR-99-37

98895

ELASTIC AND QUASI-ELASTIC pp SCATTERING IN ^{6}LiH AND ^{6}LiD TARGETS BETWEEN 1.1 AND 2.4 GeV

J. Ball[1,2], C.E. Allgower[3], M. Beddo[3a], J. Bystrický[2], M. Combet[1,2],
Ph. Demierre[4], G. Durand[2], J.-M. Fontaine[1,2], D. Grosnick[3b], R. Hess[4†],
Z. Janout[5c], Z.F. Janout[4d], V.A. Kalinnikov[5], T.E. Kasprzyk[3], B.A. Khachaturov[5],
R. Kunne[1,e], F.Lehar[2], A. de Lesquen[2], D. Lopiano[3], V.N. Matafonov[5],
I.L. Pisarev[5], A.A. Popov[5], A.N. Prokofiev[6], D. Rapin[4], J.-L. Sans[1,f],
H.M. Spinka[3], Yu.A. Usov[5], V.V. Vikhrov[6], B. Vuaridel[4], and A.A. Zhdanov[6]

1) Laboratoire National Saturne, CNRS/IN2P3 and CEA/DSM, CEA/Saclay, 91191 Gif sur Yvette Cedex, France,
2) DAPNIA, CEA/Saclay, 91191 Gif sur Yvette Cedex, France,
3) Argonne National Laboratory, HEP Division, 9700 South Cass Avenue, Argonne, IL 60439, USA,
4) DPNC, University of Geneva, 24 quai Ernest-Ansermet, 1211 Geneva 4, Switzerland,
5) Laboratory of Nuclear Problems, JINR, 141980 Dubna, Moscow Region, Russia,
6) Petersburg Nuclear Physics Institute, 188350, Gatchina, Russia,
†) Deceased.

Present address:

a) Data Ventura, LLC, Los Alamos, NM 87544, USA,
b) Dept. of Physics and Astronomy, Valparaiso Univ., Valparaiso, IN 46383, USA,
c) Faculty of Nuclear Sciences and Physical Engineering, Czech Technical University, Břehová 7, 11519 Prague 1, Czech Republic,
d) Computing Center of the Czech Technical University, Zikova 4, 16635 Prague 6, Czech Republic,
e) Institut de Physique Nucléaire IN2P3, 91400 Orsay, France,
f) Centrale Themis, F-66121 Targasonne, France.

---

* Work supported in part by the U.S. Department of Energy, Division of High Energy Physics, Contract W-31-109-ENG-38.

ABSTRACT

A polarized proton beam extracted from SATURNE II, the Saclay polarized target with ^6Li compounds, and a CH_2 target were used to measure elastic and quasi-elastic pp spin-dependent observables in the angular region $60° < \theta_{CM} < 105°$. The beam and/or target polarizations were oriented vertically. Accurate pp data for the analyzing power A_{oono}, spin correlation parameter A_{oonn}, and the polarization transfer K_{onno} were measured at 1.1 GeV. The observables A_{oono} and K_{onno} were determined at other six energies between 1.6 and 2.4 GeV. At 1.6 GeV A_{oonn} was also obtained. The individual contributions from H, ^6Li, and ^6LiD were deduced. The CH_2 target provided $A_{oono}(pp)$ results on free hydrogen and on protons in carbon. The elastic and quasi-elastic observables are compared with existing data and with phase shift analyses predictions.

1. INTRODUCTION

The experiment was carried out within the Nucleon-Nucleon (NN) program at SATURNE II. The aim of the measurements was to compare elastic and quasi-elastic spin-dependent observables in order to extend the energy region of proton-neutron data. For this purpose the new polarizable target materials ^6LiD and ^6LiH were used, and the scattering of polarized protons on protons and neutrons in ^6Li and D was studied. The pp results are presented here, while the following paper contains the np data. An unpolarized CH_2 reference target was positioned behind the main target, and scattering of polarized protons on hydrogen and on bound nucleons in carbon was measured.

The kinetic energy of 1.1 GeV is close to the highest energy of free quasi-monoenergetic polarized neutrons that can be achieved at SATURNE II. There exist complete sets of elastic pp and np observables [1,2,3] as well as the phase shift analyses (PSA) [2,4,5]. For this reason accurate measurements were performed at this energy. At six other energies the analyzing power $A_{oono}(pp)$ and the polarization transfer parameter $K_{onno}(pp)$ were measured. At 1.1 and 1.6 GeV the spin correlation parameter A_{oonn} was also determined.

Section 2 briefly describes the way the observables were extracted from the recorded data. As many items are common for pp, np, and pn observables, the relevant formulae will be omitted in the pn paper. In Section 3 we discuss the existing database for pp observables in the measured energy region. Section 4 is devoted to the beam polarimeters. In Section 5 improvements related to the Saclay polarized target are treated. Section 6 describes the experimental set-up and off-line analysis. The results are presented in Section 7. They are compared with the existing data and with fits of the Saclay-Geneva PSA (SG-PSA) at fixed energies [2,4] and with the energy dependent PSA of the Virginia Polytechnic Institute [5] (VPI-PSA).

Throughout the paper we use the NN formalism and the four-index notation for observables given in Ref.[6]. Between the notation of Ref.[5] and that of Halsen-Thomas [7,8] the following relations hold for the dominant observables treated here: $A_{oono} = A_{ooon} = P_{nooo} = P_{onoo} = P$, $A_{oonn} = C_{NN}$, $K_{onno} = K_{noon} = K_{NN}$, $D_{onon} = D_{nono} = D_{NN}$, and $N_{onnn} = N_{nonn} = H_{NNN}$.

2. DETERMINATION OF OBSERVABLES

The exact formalism for similar experiments was recently described in Ref.[9] and only necessary items will be mentioned here. The subscripts of any observable X_{srbt} refer to the polarization states of the scattered, recoil, beam, and target particles, respectively. The polarizations of the incident and target particles in the laboratory system are oriented along the basic unit vectors

$$\vec{k}, \qquad \vec{n} = [\vec{k} \times \vec{k}\,'], \qquad \vec{s} = [\vec{n} \times \vec{k}], \tag{2.1}$$

where $\vec{k}$ and $\vec{k}'$ are the beam and scattered particle directions, respectively, and $\vec{n}$ is the normal to the first scattering plane.

The scattered protons are analyzed in the directions $\vec{k}\,'$, $\vec{n}$, $\vec{s}\,' = [\vec{n} \times \vec{k}\,']$ and the recoil ones in the directions $\vec{k}''$, $\vec{n}$, $\vec{s}\,'' = [\vec{n} \times \vec{k}'']$, where $\vec{k}''$ is oriented along the recoil particle direction.

In the present experiment the beam and target polarizations ($\vec{P}_B$ and $\vec{P}_T$) were oriented vertically. Neglecting the small azimuthal angle ϕ acceptance of the apparatus, the vertical direction is parallel or antiparallel to $\vec{n}$ and the scattering plane is horizontal. This means that the most general formula for the correlated nucleon-nucleon scattering cross section Σ, as given in [6], considerably simplifies. Taking into account the generalized Pauli principle, time-reversal, and parity conservation, the single scattering term reduces to:

$$\frac{d\sigma}{d\Omega} = (\frac{d\sigma}{d\Omega})_0 \Big(1 + A_{oono}P_B + A_{ooon}P_T + A_{oonn}P_B P_T\Big), \tag{2.2}$$

where $(d\sigma/d\Omega)_0$ is the differential cross section for single scattering of unpolarized incident and target particles. It depends, as well as all observables, on the single scattering angle θ_{CM}.

The polarization of protons, outgoing from the target, was determined in the second scattering on a carbon analyzer. The asymmetry in the pC reaction with one outgoing charged particle was measured. For a given first scattering angular bin, this asymmetry depends on the proton energy T_2, on the second scattering angle θ_C, and on the azimuthal angle ϕ_C.

Due to conservation laws and in the absence of a magnetic field between the first and second scattering targets, the longitudinal component of singly-scattered protons cannot be determined. For any double scattering experiment cross section we have

$$\Sigma(P_B,P_T,A_C) = I_C\Big((\frac{d\sigma}{d\Omega}) + (\frac{d\sigma}{d\Omega})_0\ R\Big), \tag{2.3}$$

where I_C and A_C are the differential cross section and the analyzing power of the pC reaction, respectively, $d\sigma/d\Omega$ and $(d\sigma/d\Omega)_0$ were defined in Eq. (2.2), and R is the spin-dependent second scattering term. With the set-up used, only the recoil proton polarization was analyzed and the first spin-index s was zero. Under the simplified conditions given above, R reduces to

$$R(pp) = A_C\ \cos\phi_C\ \Big(P_{onoo} + K_{onno}P_B + D_{onon}P_T + N_{onnn}P_B P_T\Big). \tag{2.4}$$

For the measurements with an unpolarized target, the observables containing the target spin-index t vanish and only A_{oono} in Eq. (2.2), as well as P_{onoo} and K_{onno} in Eq. (2.4) survive.

In scattering of non-identical particles the scattered particle is taken to be the same as the incident beam one. In our case of $pn \rightarrow pn$ this is the outgoing proton, and the recoil neutron spin-index r is zero. The term $R(pn)$ reduces to:

$$R(pn) = A_C\ \cos\phi_C\ \Big(P_{nooo} + D_{nono}P_B + K_{noon}P_T + M_{nonn}P_B P_T\Big). \tag{2.5}$$

An unpolarized target therefore provides A_{oono}, P_{nooo}, and D_{nono}.

In the previous formulae we assumed $cos\phi \sim cos^2\phi \sim 1$. In fact, the ϕ acceptance of our apparatus was ±8°, whereas ϕ_C can have any value in the interval $0° - 360°$. This was taken into account in the calculations. The mean value of $< \sin^2 \phi > \sim 0.007$ introduces a negligibly small amount of A_{ooss} into A_{oonn}. Due to the ϕ-symmetry of the acceptance, $< \sin\phi > \sim 0$ and some remaining undesired observables cancel in the measurements.

The deflection of protons in the weak vertical magnetic field of the target holding coil (Section 5) conserves the vertical polarization direction. However the fringe fields may rotate the spins of beam, scattered, and recoil charged particles. This causes small contributions of other observables, but the dominant quantities remained unaffected. The P_B contribution, perpendicular to the beam direction, was calculated using the target field map and was smaller than $0.02 \cdot P_B$. The longitudinal component was found to be zero.

The field disturbs the ϕ-symmetry of the acceptance. A term $\epsilon(instr.) \cdot \sin\phi$, added in Eq. (2.2), accounted for this small instrumental effect.

At a given energy, Eq. (2.2) provides four relations for two opposite directions of $\vec{P}_B$ and $\vec{P}_T$, respectively. Only the opposite proton beam polarizations at SATURNE II for the two ion source polarized states were used. In a dedicated experiment [10] it was found that $P_B = |P_B^+| = |P_B^-|$. On the other hand $|P_T^+| \neq |P_T^-|$, but each P_T was measured by the same apparatus and a possible normalization error results in a common factor F, which multiplies both P_T^+ and P_T^-.

The conservation laws imply $A_{oono} = A_{ooon} = P_{nooo} = P_{onoo} = M_{nonn} = N_{onnn}$; these conditions were used in the data analysis. The observable $K_{onno}(pp)$ at the angle θ_{CM} is equal to $D_{onon}(pp)$ at the angle $180° - \theta_{CM}$. However this condition was not imposed and was used for data presentations in figures only.

3. EXISTING ELASTIC AND QUASI-ELASTIC pp DATA

In Table 1 we give a list of the existing elastic and quasi-elastic $A_{oono} = A_{ooon}$ and A_{oonn} *pp* data measured between 1.0 and 2.5 GeV [11-34]. They can be compared with the present results. The data in Ref.[17] are preliminary only, but the final results are available and will be published. The data from Ref.[33] were measured with an internal target at $\theta_{lab} = 68°$. Accurate A_{ooon} measurements below 2.5 GeV with an unpolarized proton beam and a polarized atomic hydrogen jet were recently performed at COSY. The data are not available yet.

The A_{oono} data measured before 1983 were fitted and analyzed in Ref.[35]. In the energy region under discussion, the authors observed a considerable difference in the absolute polarization values between the different data sets. Common fits averaging these sets suggested to normalize the data in Refs. [23,29,30] downward by 10 %, 8 %, and 8 %, respectively. The data in Refs. [28,32] needed to be normalized upwards by 15 % and 12 %. PSA fits including the SATURNE II data give similar conclusions as in Ref.[35].

In the energy region under discussion, $K_{onno}(pp)$ and $D_{onon}(pp)$ were measured at SATURNE II from 0.995 to 2.396 GeV at 7 energies [36,37,38], from 1.80 to 2.10 GeV at four energies [39], and between 1.975 and 2.495 GeV at 20 energies [9]. For "pure" observables, 302 data points were obtained. In other laboratories one point was measured at 1.90 GeV at the BNL COSMOTRON [40] and three points were determined at 2.205 GeV at the ANL-ZGS [41].

4. BEAM POLARIMETERS

The vertical polarization of the extracted proton beam at SATURNE II was flipped at each accelerator spill. The extracted beam polarization was monitored by a beam line polarimeter PL1 [42,43], which had two pairs of kinematically conjugate arms in the horizontal plane and beam intensity monitors in the vertical plane.

Downstream of PL1 the beam passed through three thin windows, and through the target of the second beam polarimeter (PL2), before entering the polarized target. The outgoing beam passed through the CH_2 target, 10 mm thick and 15 mm in diameter, placed 16 cm downstream from the polarized target.

The PL2 polarimeter, positioned $\sim$ 2.5 m upstream of the polarized target, measured left-right (L-R) and up-down (U-D) scattering asymmetries [42,44]. The absence of a horizontal beam polarization component resulted in a zero U-D asymmetry.

A third polarimeter (PL3), that measured the L-R asymmetry, was positioned 6.54 m downstream of PL2 on a remotely-controlled movable table. The PL3 array could move horizontally, perpendicular to the beam axis [39].

The proton beam energy at the PL1 target was the same as the nominal extracted beam energy with a spread smaller than 200 keV. The beam at the polarized target center lost about 5 MeV with respect to the nominal accelerator energy. The beam energy at the CH_2 target was 8 to 9 MeV smaller than the nominal value. The energy spread was $\sim \pm$ 0.4 MeV in the PL1 target, $\sim \pm$ 3.5 MeV in the polarized target, and $\sim \pm$ 0.9 MeV in the CH_2 target. The spread decreased only slightly with increasing energy.

5. POLARIZED TARGET

The ^6LiD material contained protons in ^6Li, in D, and in a small amount of residual hydrogen. The ^6Li, D, and H nuclei are polarized in ^6LiH and ^6LiD targets. It has been observed that ^6Li behaves as $^4He + D$, where only the deuterons are polarized [45]. This decreases the fraction of polarized protons or neutrons in ^6Li to 1/3. We have taken $\omega_D = 0.05$ for the probability of the deuteron to be in a D state, in agreement with the majority of calculated values [46]. Then the polarizations of protons P_p and neutrons P_n in deuterons are related to the deuteron polarization P_d by $P_p = P_n = P_d(1 - 1.5\,\omega_D)$.

In order to polarize the ^6Li compounds, paramagnetic centers must be created by electron irradiation of these materials at a temperature close to liquid nitrogen. The target polarization obtained in a given magnetic field depends on the irradiation dose, time, precise temperature, and the purity of the material. The target polarization measurement by the NMR method is more accurate than for deuterated aliphatic alcohols or deuterated ammonia. Due to the crystaline structure of ^6Li compounds, the NMR spectra show simple resonance behaviour, similarly to polarized proton targets with doped butanol or pentanol. The development of this kind of target has been described in Refs. [46,47,48].

In the compounds ^6LiH and ^6LiD only the polarization of the protons and the deuterons, respectively, was measured. We assumed that Equal Spin Temperature conditions were present. This means that the measurement of the polarization of one element enabled us to deduce the polarizations of the others [48].

To separate the effects from ^6Li and from D, a calibration with ^6LiH is needed. This material has been specially prepared in St.Petersburg (Russia). For the purpose of the present experiment, two new target containers for the Saclay frozen spin target [47] were constructed. Both were 45 mm thick (in the beam direction) and 20 mm in diameter. They were inserted in the same refrigerator. The distance between the container axes was 3.0 cm vertically. One of them contained ^6LiD and one ^6LiH materials. This construction allowed either of the targets to be polarized and inserted in the beam without the opening of the cryostat. Both targets were polarized in the homogenous magnetic field of 2.5 Tesla. The deuteron polarization build-up time was around 8 hours.

When the maximum polarization was reached, the target was set into the frozen spin mode. Scattering measurements were performed in the holding field of 0.33 Tesla at the target center, provided by a vertical superconducting holding coil [47]. Under these conditions the relaxation time of the targets averaged around 12 days.

The hydrogen polarizations in the ^6LiH target at 1.1 GeV were $\sim +27$ % and ~ -30 %, respectively. The deuteron polarizations in ^6LiD at 1.1 and 1.6 GeV were $\sim +5$ % and ~ -17 %. Considerably higher P_T values were obtained in different tests [47]. Unfortunately, due to a failure of the electricity, the target polarization was lost and could not be re-established. At energies between 1.8 and 2.4 GeV the targets were unpolarized.

6. EXPERIMENTAL SET-UP AND OFF-LINE ANALYSIS

The present measurements were carried out using the Nucleon-Nucleon experimental set-up. This apparatus is described in detail in Ref.[44]. It consisted of a two-arm spectrometer with an analyzing magnet and a neutron counter (NC) hodoscope in the forward arm. The NC hodoscope was preceeded by four "veto" counters, not used for *pp* events. Each arm was equipped with single scintillation counters and counter hodoscopes. Signals from these counters triggered eight multi-wire proportional chambers (MWPC's) with three wire planes each.

The *pp* triggers were selected by the coincidence of charged particles in both arms. The scintillation counters also measured time-of-flight (TOF). The forward proton momenta were analyzed by a dipole magnet and by TOF.

The recoil protons were rescattered on a 6 cm-thick carbon analyzer and L-R and U-D rescattering events were recorded by the MWPC's.

The acceptance of each arm in the laboratory frame was $\sim \pm 4.5°$ vertically and 23° horizontally. The ϕ acceptance of both arms together was limited to $\pm 8°$.

Complete tracking was performed for each recorded event. For the first scattering this provided the vertex position in the target, the scattering and azimuthal angles

θ_1, ϕ_1, θ_2, ϕ_2, the TOF, and the momentum of the forward charged particle.

For investigation of the elastic events in ^6LiH, a cut of ±2.5° was applied on $\Delta\theta_{CM}$ and $\Delta\phi$, together with cuts on the vertex position, TOF, and $\Delta p_{scatt.}$ [44]. The quasi-elastic contribution from ^6Li and inelastic events were subtracted using the wings of the ϕ distribution. The background was on the order of 6 %.

The same cuts on TOF and $\Delta p_{scatt.}$ were applied for the study of ^6LiD and ^6Li in ^6LiH. The H events in ^6LiH were suppressed by removing the central part of the $\Delta\theta_{CM}$ and $\Delta\phi$ distributions. In order to reduce the inelastic contribution as much as possible, the cuts in the space $\Delta\theta_{CM}$ and $\Delta\phi$ were enlarged to a circle of radius 10° only. For ^6Li in the ^6LiH target this contribution was estimated to be smaller than 2 % at 1.1 GeV and less than 7 % at 2.4 GeV. For the entire ^6LiD target the inelastic contamination varied from 1 % to 4 %, respectively. The cryogenic envelope contributed at the level of $\sim$ 1 % to the number of events. It was taken into account as a dilution of the $|P_T|$ value.

The $\Delta\theta_{CM}$ distribution for *pp* events in the ^6LiH target is shown in Fig. 1. It contains a narrow hydrogen peak and the broad and asymmetric distribution from the quasi-elastic *pp* events in ^6Li. Subtracting the events on hydrogen one obtains the contribution from ^6Li. These events are statistically independent of those for elastic *pp* scattering on H in the same target. Both sets of the data may be used in any data analysis (e.g. PSA).

The shape of the $\Delta\theta_{CM}$ distribution for *pp*, using the ^6LiD target, is shown in the same figure. The small hydrogen peak is due to the residual hydrogen present in this target. The subtraction of ^6Li events from ^6LiD events gives the quasi-elastic *pp* effect from D.

In tables we present the *pp* elastic data, the quasi-elastic ones from pure ^6Li, and the results from the entire ^6LiD target. These last data are the most interesting for any future use of ^6LiD.

The cuts change the relative trigger contributions from the target components. At 1.1 and 1.6 GeV for *pp* single scattering in the ^6LiD material we had 52 % of effective triggers from ^6Li, 44 % from D, and 4 % from residual hydrogen. At the higher energies a different target material was used and the hydrogen events represented $\sim$ 15%.

Since no ^6LiH data exist at 1.6 GeV, the individual triggers were obtained by comparing the Monte Carlo acceptances for ^6Li and D at 1.1 and 1.6 GeV. We have used the Hulthen distribution $H\ (p_f)$ of the Fermi momentum p_f for bound nucleons in the deuteron :

$$H\ (p_f) = \frac{p_f^2}{(p_f^2 + \alpha^2)^2 \times (p_f^2 + \beta^2)^2} \tag{6.1}$$

with $\alpha = 0.045$ GeV/c and $\beta = 0.270$ GeV/c. We have used a Hulthen-like distribution for ^6Li with $\alpha = 0.160$ GeV/c and $\beta = 0.200$ GeV/c, and for carbon with $\alpha = 0.225$ GeV/c and $\beta = 0.227$ GeV/c. These functions described fairly well all observed distributions. This can be seen for ^6Li Monte Carlo simulation in Fig.1. At 1.1 GeV the comparison of ^6LiH and ^6LiD data with the Monte Carlo simulation are consistent with a shadowing effect of ~ 0.8 on ^6Li.

From the set of single scattering events, those with one charged particle outgoing from the carbon analyzer were selected. The vertex in carbon, as well as the angles of the rescattered particle θ_C and ϕ_C were determined.

Cuts were applied on the vertex in carbon, on $\Delta\theta_C$, as well as for the $\Delta\phi_C$ and ϕ mirror symmetry conditions [44]. The remaining events at all energies represented about 2 % of the selected single scattering events.

From the first and second scattering vertices the energy losses in the PPT and carbon targets were calculated and gave the recoil particle energy T_2. The T_2 and θ_C values on the carbon analyzer were used to determine the corresponding A_C value for each accepted event.

The proton-carbon asymmetry is measured for only one outgoing charged particle. The $p - C$ analyzing power A_C for this reaction was interpolated from existing results. This procedure was discussed in detail in our preceeding paper [39], where an exhaustive list of relevant references is given that will be omitted here. The interpolated A_C values introduce a relative error of ±6 % in the rescattering observables at all energies. These observables were determined using the method first proposed by the Geneva group [49]; see also Ref.[50].

The CH_2 target, downstream from the polarized target, measured *pp* single scattering on free protons and on protons in carbon nuclei. The triggers for *pp* scattering events from the CH_2 target were independent from those used for the polarized target. Events were recorded by the same apparatus and analyzed using the same criteria as for the *pp* scattering events.

The simultaneous measurements of scattering on a polarized and on an unpolarized target is used to check the normalization of events recorded during two opposite target polarizations. This is necessary due to the fact that the P_T was reversed after several hours of data taking, compared to the $\vec{P}_B$ flip at every spill.

The CH_2 target provided A_{oono} *pp* elastic scattering on hydrogen and quasi-elastic scattering on protons in carbon. The same method, as described above, was performed to deduce the *pp* quasi-elastic scattering on strongly bound carbon protons. The two sets of the results are again statistically independent, but the carbon data are more affected by inelastic reactions than the ^6Li data.

7. RESULTS AND DISCUSSION

The results are given with beam energies corresponding to those at the target centers. Independent data obtained in the elastic scattering of protons on H in ^6LiH and in CH_2 targets are listed in the tables. Also, quasi-elastic data on $^6Li + D$ $(+H)$ in the ^6LiD target, together with those on ^6Li and C are tabulated. Due to the large amount of results, in several figures only the H and ^6LiD data could be plotted. The quoted errors in the tables and the figures are statistical ones. The relative normalization error of P_B was ±3 %, that of P_T was ±4 % at 1.1 GeV and up to ±10 % at 1.6 GeV.

The predictions of two PSA at all energies are plotted in the figures. The independent data for all observables at 1.1 GeV were included into the SG-PSA with their statistical errors. The SG-PSA at other energies and the VPI-PSA at all energies were carried out using the previously existing data only.

In Table 2 are listed the independent A_{oono} results at all energies measured with the ^6LiH and ^6LiD targets. Measurements at 1.6 GeV were carried out with the ^6LiD target only. All the independent results are plotted in Fig. 2, and the H and ^6LiD data are shown in Figs. 3 to 5. A significative part of previously measured SATURNE II data is also plotted. We observe an excellent agreement of elastic and quasi-elastic results. Fig. 2 shows that the new data at 1.1 GeV improve considerably the accuracy of the Saclay data set above $\theta_{CM} = 43.4°$ [11].

In Table 3 are given the elastic and quasi-elastic pp data obtained with the CH_2 target. For 1.1 GeV they are plotted in Fig. 6 together with the PSA predictions.

Note that $A_{oono}(pp)$ in the interval $0° < \theta_{CM} < 90°$ reaches its first minimum at $-t \sim 1.0$ (GeV/c)^2. This was observed for all available data up to 200 GeV and described in Ref.[51]. Additional examples are given in Ref.[52]. Around 1.1 GeV this minimum is close to $\theta_{CM} = 90°$ and A_{oono} as a function of θ_{CM} changes rapidly with energy. For this reason, only the A_{oono} data measured very close to 1.1 GeV are shown in Fig. 2.

The SG-PSA fits to all existing data at 1.0, 1.1, and 1.3 GeV are shown in Fig. 7. The accurate elastic ANL-ZGS results [26] at 1.030 GeV are well described by the fit at 1.0 GeV. Its angular dependence is closer to a sinusoidal shape, with respect to the fit at 1.1 GeV. Two previous experiments suggested strong variation of the A_{oono} angular dependence and even negative A_{oono} values at large angles above 1.1 GeV: the SATURNE I data at 1.194 ± 0.008 GeV [21], and CERN data at 1.181 ± 0.017 GeV [24]. This was confirmed by the SATURNE II measurements at 1.295 GeV [12], where the A_{oono} values in the region $75° \leq \theta_{CM} < 90°$ are negative. The former energy dependent SG-PSA [53] described this fact well. Since in the interval around 1.1 GeV, $A_{oono}(pp)$ is very sensitive to small energy variations, the excellent agreement of the independent results suggests that no Glauber-type corrections for the quasi-elastic data are needed.

Up to 1.8 GeV at large angles, the A_{oono} values are close to zero as can be seen in Fig. 3. The minimum at $-t \sim 1.0$ (GeV/c)^2 in ANL-ZGS data sets [25,26,29,30] and in the VPI-PSA predictions is well pronounced only above 2.2 GeV. At this energy the minimal values are positive and the position of the minimum moves below 60° (see Figs. 4, 5).

The spin correlation parameter $A_{oonn}(pp)$ results at two energies are listed in Table 4. At 1.1 GeV the free data were accurately determined using the ^6LiH target. The errors are larger for the measurements with the ^6LiD target due to the small $|P_T|$ values. The results on ^6Li have large errors and were omitted. The data at two energies are plotted in Fig. 8. The new data at 1.1 GeV smoothly connect with the SATURNE II results at small angles [34], are in good agreement with all ANL-ZGS data at 1.047 Gev [30], and with the previous Saclay data above $\theta_{CM} = 63°$ [11]. Below this angle eight points from [11] differ within two statistical errors. The

SG-PSA correctly describes all existing data and is in agreement with the VPI-PSA predictions.

At 1.6 GeV the two PSA predictions for A_{oonn} differ. The SG-PSA includes the SATURNE II points measured at the same energy. The VPI-PSA is affected by former ANL data at other energies with large uncertainties in energy and in P_B normalizations (see ref.[35]).

The pp rescattering observables D_{onon} and K_{onno} are given in Tables 5 and 6, respectively. The H and ^6Li data at six lower energies are presented in Fig. 9 using the equality $K_{onno}(\pi - \theta_{CM}) = D_{onon}(\theta_{CM})$. They are compared with the previous SATURNE II data [9,36–39], with the BNL point at 1.90 GeV [40], and with the three ANL points at 2.205 GeV [41]. We observe a good agreement of all new K_{onno} results plotted at large angles. This quantity depends on the large $|P_B|$ values only. The D_{onon} points at 1.1 GeV, depending on the relatively small P_T values, are more dispersed. Note that the number of events was at least 50 times smaller than for single scattering. We observe a good agreement with the majority of the existing data points and the two PSA predictions. The data at 1.6 and 1.8 GeV were obtained with the ^6LiD target only. The ^6LiH target was not used at 1.6 GeV. The statistics of K_{onno} events, recorded with this target at 1.8 GeV, was very small and the results were omitted. At 2.4 GeV only two points with large errors were obtained and they are listed in Table 6.

8. CONCLUSIONS

Quasi-elastic scattering of protons on weakly bound protons in deuterons and in ^6Li nuclei shows agreement with elastic scattering results for all measured observables. The equality of elastic and quasi-elastic scattering data suggests that ^6LiD is an excellent target for experiments with polarized nucleons. It also suggests that no additional corrections to spin-dependent $pp \rightarrow pp$ data are needed. The quasi-elastic scattering on strongly bound nucleons in carbon nuclei is more dependent on cuts.

The present results at 1.1 GeV improve significantly our knowledge of analyzing power, spin correlation parameter, and rescattering observable angular dependence. At higher energies the new data supplement the existing database. Since the pp PSA below 2.4 GeV is still fairly well constrained, the comparison of predictions with the new elastic and quasi-elasic pp results is significant.

ACKNOWLEDGEMENTS

The SG-PSA fits were carried out with a help of C. Lechanoine-Leluc. We express our gratitude to R.A.Arndt and I.I.Strakovsky for the recent VPI-PSA predictions. We also thank the well organized SATURNE II operations crew for their help. This work was supported in part by the U.S. Department of Energy, Division of Nuclear Physics, Contract No. W-31-109-ENG-38, by the Swiss National Science Foundation, and by the Russian Foundation for Fundamental Nuclear Physics Programme 122.03.

REFERENCES

[1] C.D. Lac, J. Ball, J. Bystrický, J. Derégel, F.Lehar, A. de Lesquen, L. van Rossum, J.-M. Fontaine, F. Perrot, and P.Winternitz, J.Phys. France **51** (1990) 2689.

[2] J.Bystrický, C.Lechanoine-LeLuc, and F.Lehar, Eur. Phys. J. **C4** (1998) 607.

[3] J. Ball, J. Bystrický, J.-M. Fontaine, G. Gaillard, R. Hess, Z. Janout, B.A. Khachaturov, R. Kunne, C.D. Lac, C. Lechanoine-Leluc, F. Lehar, A. de Lesquen, D. Lopiano, F. Perrot-Kunne, D. Rapin, L. van Rossum, H. Schmitt, and H.M. Spinka, Nuovo Cimento **A111** (1998) 13.

[4] J.Bystrický, C. Lechanoine-Leluc, and F.Lehar, J.Phys. France **51** (1990) 2747.

[5] R.A.Arndt, C.H. Oh, I.I. Strakovsky, R.L. Workman, and F. Dohrman, Phys.Rev. **C56** (1997) 3005, SAID solution SP99.

[6] J. Bystrický, F. Lehar, and P. Winternitz, J.Physique (Paris) **39** (1978) 1.

[7] F. Halzen and G.H.Thomas, Phys.Rev. **D10** (1974) 344.

[8] I.P.Auer, J.Chalmers, E.Colton, R.Giese, H.Halpern, D.Hill, R.Miller, K.Nield, B.Sandler, H.Spinka, N.Tamura, D.Underwood, Y.Watanabe, A.Yokosawa, A.Beretvas, and D.Miller, Phys.Rev. **D32** (1985) 1609.

[9] C.E. Allgower, J. Ball, L.S. Barabash, M. Beddo, Y. Bedfer, A. Boutefnouchet, J. Bystrický, P.-A. Chamouard, Ph. Demierre, J.-M. Fontaine, V. Ghazikhanian, D. Grosnick, R. Hess, Z. Janout, Z.F. Janout, V.A. Kalinnikov, T.E. Kasprzyk, Yu.M. Kazarinov, B.A. Khachaturov, R. Kunne, C. Lechanoine-LeLuc, F. Lehar, A. de Lesquen, D. Lopiano, M. de Mali, V.N. Matafonov, I.L. Pisarev, A.A. Popov, A.N. Prokofiev, D. Rapin, J.-L. Sans, H.M. Spinka, Yu.A. Usov, V.V. Vikhrov, B. Vuaridel, C.A. Whitten, and A.A. Zhdanov, Eur.Phys.J. **C5** (1998) 453.

[10] Ch. Allgower, J. Arvieux, P. Ausset, J. Ball, P.-Y. Beauvais, Y. Bedfer, J. Bystrický, P.-A. Chamouard, Ph. Demiere, J.-M. Fontaine, Z. Janout, V.A.Kalinnikov, T.E.Kasprzyk, B.A.Khachaturov, R. Kunne, J.-M.Lagniel, F. Lehar, A. de Lesquen, A.A.Popov, A.N. Prokofiev, D. Rapin, J.-L. Sans, H.M. Spinka, A. Teglia, V.V. Vikhrov, and A.A. Zhdanov, Nucl.Instrum.Methods **A399** (1997) 171.

[11] J. Bystrický, P. Chaumette, J. Derégel, J. Fabre, F. Lehar, A. de Lesquen, F. Petit, L. van Rossum, J.-M. Fontaine, F. Perrot, J. Ball, A. Michalowicz, Y. Onel, and A. Penzo, Nucl.Phys. **B262** (1985) 715.

[12] F.Perrot, J.-M.Fontaine, F.Lehar, A. de Lesquen, J.P.Meyer, L. van Rossum, P.Chaumette, J.Derégel, J.Fabre, J.Ball, C.D.Lac, A.Michalowicz, Y.Onel, B.Aas, D.Adams, J.Bystrický, V.Ghazikhanian, G.Igo, F.Sperisen, C.A.Whitten, and A.Penzo, Nucl.Phys. **B294** (1987) 1001.

[13] C.E. Allgower, J.Ball, M.Beddo, Y.Bedfer, A.Boutefnouchet, J.Bystrický, P.-A. Chamouard, Ph. Demierre, J.-M. Fontaine, V. Ghazikhanian, D. Grosnick, R.Hess, Z.Janout, Z.F. Janout, V.A.Kalinnikov, T.E.Kasprzyk, B.A. Khachaturov, R.Kunne, F.Lehar, A. de Lesquen, D.Lopiano, V.N. Matafonov, I.L.Pisarev, A.A.Popov, A.N. Prokofiev, D.Rapin, J.-L.Sans, H.M.Spinka, A.Teglia, Yu.A.Usov, V.V.Vikhrov, B.Vuaridel, C.A.Whitten, and A.A.Zhdanov, Nucl.Phys. **A637** (1998) 231.

[14] J. Arvieux, J. Ball, J. Bystrický, J.-M. Fontaine, G. Gaillard, J.P. Goudour, R. Hess, R. Kunne, F. Lehar, A. de Lesquen, D. Lopiano, M. de Mali, F. Perrot-Kunne, D. Rapin, L. van Rossum, J.-L. Sans, and H.M. Spinka, Zeitschrift für Physik **C76** (1997) 465.

[15] J. Ball, M. Beddo, Y. Bedfer, J. Bystrický, P.-A. Chamouard, M. Combet, Ph. Demierre, J.-M. Fontaine, G. Gaillard, D. Grosnick, R. Hess, R. Kunne, F.Lehar, A. de Lesquen, D. Lopiano, D. Rapin, J.-L. Sans, and H.M. Spinka, submitted to Eur.Phys.J. C .

[16] J. Ball, V. Ghazikhanian, J. Gordon, F. Lehar, A. de Lesquen, F. Perrot, and L. van Rossum, Nucl.Phys. **B286** (1987) 635

[17] C.E.Allgower, PhD thesis, ANL-HEP-TR-97-71, August 1997

[18] M.Garçon, J.C.Duchazeaubeinex, J.C.Faivre, B.Guillerminet, D.Legrand, M.Rouger, J.Saudinos, and J.Arvieux, Phys.Lett. **B183** (1987) 273.

[19] S.Dalla Torre-Colautti, R.Birsa, F.Bradamante, M.Giorgi, L.Lanceri, A.Martin, A.Penzo, P.Shiavon, V.Sossi, A.Villari, H.Azaiez, K.Kuroda, A.Michalowicz, and F.Lehar, Nucl.Phys. **A505** (1989) 561.

[20] P.Bareyre, J.F.Detoeuf, L.W.Smith, R.D.Tripp, and L. van Rossum, Nuovo Cimento **20** (1961) 1049.

[21] G.Cozzika, Y.Ducros, A. de Lesquen, J.Movchet, J.C.Raoul, L. van Rossum, J.Derégel, and J.-M.Fontaine, Phys.Rev. **164** (1967) 1672.

[22] H.A.Neal and M.J.Longo, Phys.Rev. **161** (1967) 1374.

[23] P.Grannis, J.Arens, F.Betz, O.Chamberlain, B.Dieterle, C.Schultz, G.Shapiro, L. van Rossum, and D.Weldon, Phys.Rev. **148** (1966) 1297.

[24] M.G.Albrow, S.Andersson/Almehed, B.Bosniakovic, C.Daum, F.C.Erne, J.P.Lagnaux, J.C.Sens, and F.Udo, Nucl.Phys. **B23** (1970) 445.

[25] V.V.Zhurkin, I.M. Ivanchenko, V.P. Kanavets, N.N. Karpenko, I.I. Levintov, V.I. Martynov, O.E. Mikhailov, B.V. Morozov, V.M. Nesterov, I.I. Pershin, L.M. Polyakova, V.V. Ryltsov, and T.S.Cherkalina, Yad.Fiz. **28** (1978) 1280 and Sov.J.Nucl.Phys **28** (1978) 660.

[26] M.L. Marshak, E.A. Peterson, K. Ruddick, J. Lesikar, T. Mulera, J.B. Roberts, R.D. Klem, R. Talaga, and A. Wriekat, Phys. Rev. **C18** (1978) 331.

[27] D.Miller, C.Wilson, R.Giese, D.Hill, K.Nield, P.Rynes, B.Sandler, and A.Yokosawa, Phys.Rev. **D16** (1977) 2016.

[28] J.H.Parry, N.E.Booth, G.Conforto, R.J.Esterling, J.Scheid, D.J.Sherden, and A.Yokosawa, Phys.Rev. **D8** (1973) 45.

[29] A.Lin, J.R.O'Fallon, L.G.Ratner, P.F.Schultz, K.Abe, D.G.Crabb, R.C.Fernow, A.D.Krisch, A.J.Salthouse, B.Sandler, and K.M.Terwilliger, Phys.Lett. **74B** (1978) 273.

[30] D.A.Bell, J.A. Buchanan, M.M. Calkin, J.M. Clement, W.H. Dragoset, M. Furič, K.A.Johns, J.D. Lesikar, H.E. Miettinen, T.A. Mulera, G.S. Mutchler, G.G. Phillips, J.B. Roberts, and S.E. Turpin, Phys.Lett. **94B** (1980) 310.

[31] Y. Makdisi, M.L. Marshak, B. Mossberg, E.A. Peterson K. Ruddick, J.B. Roberts, and R.D. Klem, Phys. Rev. Lett. **45** (1980) 1529.
The numerical values exist in the thesis of Björn Mossberg from University of Minnesota.

[32] R.Diebold, D.S.Ayres, S.L.Kramer, A.J.Pawlicki, and A.B.Wicklund,

Phys.Rev.Lett. **35** (1975) 632.

[33] Y. Kobayashi, K. Kobayashi, T.Nakagawa, H. Shimizu, H.Y. Yoshida, H. Ohnuma, J.A. Holt, G. Glass, J.C. Hiebert, R.A. Kenefick, S.Nath, L.C. Northcliffe, A.J. Simon, S. Hiramatsu, Y.Mori, H.Sato, A. Takagi, T. Toyama, A.Ueno, and K. Imai, Nucl.Phys. **A569** (1994) 791.

[34] F.Lehar, A. de Lesquen, J.P.Meyer, L. van Rossum, P.Chaumette, J.Derégel, J.Fabre, J.-M.Fontaine, F.Perrot, J.Ball, C.D.Lac, A.Michalowicz, Y.Onel, D.Adams, J.Bystrický, V.Ghazikhanian, C.A.Whitten, and A.Penzo, Nucl.Phys. **B294** (1987) 1013

[35] H.Spinka, E.Colton, W.R.Ditzler, H.Halpern, K.Imai, R.Stanek, N.Tamura, G.Theodosiou, K.Toshioka, D. Underwood, R.Wagner, Y. Watanabe, A. Yokosawa, G.R. Burleson, W.B. Cottingame, S.J. Greene, S. Stuart, and J.J. Jarmer, Nucl.Instrum.Methods **211** (1983) 239.

[36] C.D.Lac, J.Ball, J.Bystrický, F.Lehar, A. de Lesquen, L. van Rossum, F.Perrot, J.-M.Fontaine, P.Chaumette, J.Derégel, J.Fabre, V.Ghazikhanian, and A.Michalowicz, Nucl.Phys. **B321** (1989) 284.

[37] C.D. Lac, J. Ball, J. Bystrický, F. Lehar, A. de Lesquen, L. van Rossum, F.Perrot, J.-M.Fontaine, P. Chaumette, J. Derégel, J.Fabre, V. Ghazikhanian, A. Michalowicz, Y.Onel, and A.Penzo, Nucl.Phys. **B315** (1989) 284.

[38] C.D.Lac, J.Ball, J.Bystrický, F.Lehar, A. de Lesquen, L. van Rossum, F.Perrot, J.-M.Fontaine, P.Chaumette, J.Derégel, J.Fabre, V.Ghazikhanian, and A.Michalowicz, Nucl.Phys. **B321** (1989) 269.

[39] C.E. Allgower, J. Ball, L.S. Barabash, M. Beddo, Y. Bedfer, A.Boutefnouchet, J.Bystrický, Ph. Demierre, J.-M. Fontaine, V. Ghazikhanian, D. Grosnick, R. Hess, Z. Janout, Z.F. Janout, V.A. Kalinnikov, T.E. Kasprzyk, Yu.M.Kazarinov, B.A.Khachaturov, R. Kunne, F.Lehar, A. de Lesquen, D. Lopiano, M. de Mali, V.N. Matafonov, I.L. Pisarev, A.A. Popov, A.N. Prokofiev, D.Rapin, J.-L. Sans, H.M. Spinka, S. Trentalange, Yu.A.Usov, V.V.Vikhrov, B.Vuaridel, C.A.Whitten, and A.A.Zhdanov, Eur.Phys.J. **C 1** (1998) 131.

[40] W.C.Carithers, Jr., R.K.Adair, C.J.B. Hawkins, H. Kasha, R.C. Larsen, L.B. Leipuner, L.W. Smith, and T.P.Wangler, Phys.Rev. **179** (1969) 1304.

[41] G.W.Abshire, G.W.Bryant, M. Corcoran, R.R. Crittenden, S.W.Gray, R.M. Heinz, A.W.Hendry, H.A. Neal, and D.R.Rust, Phys.Rev **D12** (1975) 3393.

[42] J. Bystrický, J. Derégel, F. Lehar, A. de Lesquen, L. van Rossum, J.-M. Fontaine, F. Perrot, C. A. Whitten, T. Hasegawa, C. R. Newsom, W. R. Leo, Y. Onel, S. Dalla Torre-Colautti, A. Penzo, H. Azaiez, and A. Michalowicz, Nucl. Instrum. Methods **A239** (1985) 131.

[43] M.Arignon, J.Bystrický, J.Derégel, J.-M.Fontaine, T.Hasegawa, F.Lehar, C.R.Newsom, A.Penzo, F.Perrot, L. van Rossum, C.A.Whitten, and J. Yonnet, Note CEA-N-2375, Saclay, Décembre 1983.

[44] J. Ball, Ph. Chesny, M. Combet, J.-M. Fontaine, R. Kunne, J.-L. Sans, J. Bystrický, C.D. Lac, D. Legrand, F. Lehar, A. de Lesquen, M. de Mali, F. Perrot-Kunne, L. van Rossum, P. Bach, Ph. Demierre, G. Gaillard, R. Hess, Z.F. Janout, D. Rapin, Ph. Sormani, B. Vuaridel, J.P. Goudour, R. Binz, A. Klett, E. Rössle, H. Schmitt, L.S. Barabash, Z. Janout, V.A. Kalinnikov, Yu.M. Kazarinov, B.A. Khachaturov, V.N. Matafonov, I.L. Pisarev, A.A. Popov, Yu.A. Usov, M. Beddo, D. Grosnick, T. Kasprzyk, D. Lopiano, and H. Spinka,

Nucl. Instrum. Methods **A327** (1993) 308.

[45] S. Ritt, E.T.Boschitz, R.Meier, R.Tacik, M.Wessler, K.Junker, J.A.Konter, S.Mango, D.Renker, B. van den Brandt, V.Efimovykh, A.Kovaljov, A.Prokofiev, R.Mach, P.Chaumette, J.Derégel, G.Durand, J.Fabre, and W.Thiel, Phys.Rev. **C43** (1991) 745.

[46] S. Bültmann, D.G.Crabb, D.B.Day, R.D.Fatemi, B.Gardner, C.M.Harris, J.R.Johnston, J.S. McCarthy, P.M.McKee, W.Meyer, S.I.Pentillä, E.Ponikvar, A.Rijllart, O.A.Rondon, S.St.Lorant, W.A.Tobias, S.Trentalange, H.Zhu, B.Zihlmann, and D.Zimmermann, A Study of Lithium Deuteride as a Material for a Polarized Target, Preprint SLAC-PUB-7904, August 1998, to be published.

[47] J. Ball, M. Combet, J.-L. Sans, B. Benda, P. Chaumette, J. Derégel, G. Durand, A.P. Dzyubak, C. Gaudron, F. Lehar, A. de Lesquen, T.E. Kasprzyk, Z. Janout, B.A. Khachaturov, V.N. Matafonov, and Yu.A. Usov, Nucl. Instrum. Methods **A381** (1996) 4.

[48] St.Goertz, Ch.Bradtke, H.Dutz, R.Gehring, W.Meyer, M.Plückthun, G.Reicherz, K.Runkel, and A.Thomas, Nucl. Instrum. Methods **A356** (1995) 20.

[49] D. Besset, Q.H. Do, B.Favier, L.G. Greeniaus, R.Hess, C. Lechanoine, D.Rapin, D.W. Werren, and Ch.Weddigen, Nucl.Instrum.Methods **166** (1979) 379.

[50] A. Teglia, Ph.D. Thèse No 2948, DPNC, Université de Genève, 1997.

[51] F.Lehar, A. de Lesquen, F.Perrot, and L. van Rossum, Europhysics Lett. **3** (1987) 1175.

[52] C. Lechanoine-Leluc and F.Lehar, Rev.Mod.Phys. **65** (1993) 47.

[53] F.Lehar, C.Lechanoine-Leluc, and J.Bystrický, J.Physique (Paris) **48** (1987) 1273.

TABLE CAPTIONS

Table 1 Existing spin-dependent $A_{oono}(pp) = A_{ooon}(pp)$ and $A_{oonn}(pp)$ data in the energy region from 1.0 to 2.5 GeV. The meaning of the symbols is: p pol. ... accelerated polarized protons, p scat. ... protons polarized by scattering, p ... unpolarized protons, d pol. ... polarized deuterons, Scint. ... active scintillating target, PDT ... polarized deuteron target, LH_2 ... liquid hydrogen, LD_2 ... liquid deuterium.

Table 2 The analyzing power $A_{oono} = A_{ooon}$ in scattering of polarized protons either on hydrogen in the ^6LiH target, or on bound protons in the ^6LiD target. The parentheses in $^6Li + D\ (+H)$ refer to the small amount of H in the ^6LiD target. Subtracting the hydrogen effect in ^6LiH, the contribution of protons in ^6Li was deduced. The three sets of the results are independent. Quoted errors are statistical uncertainties. The relative normalization systematic error due to the beam polarization was ±3 %.

Table 3 The pp analyzing power A_{oono} in elastic and quasi-elastic scattering on free and strongly bound protons in the CH_2 target. Quoted errors are statistical uncertainties. All results are independent. The relative normalization systematic error in P_B was ±3 %.

Table 4 The spin correlation parameter A_{oonn} in scattering of polarized protons either on polarized hydrogen in the ^6LiH target, or on polarized bound protons in the ^6LiD target. The parentheses in $^6Li + D\ (+H)$ refer to the small amount of H in the ^6LiD target. Quoted errors are statistical uncertainties. The normalization systematic error in P_B was ±3 %. At 1.095 GeV $\Delta P_T = \pm 4$ %, while at 1.595 GeV the accuracy was ±10 %.

Table 5 The observable D_{onon} for elastic scattering of polarized protons on the polarized ^6LiH target. The relative normalization systematic error in the target polarization was ±4 %. The relative systematic error provided by the normalization uncertainty in the p-C analyzing power was ±6 %. Another absolute error of ±15 % is due to the relative normalization of measurements with the two opposite (and small) P_T values.

Table 6 The observable K_{onno} measured with the polarized proton beam scattered either on hydrogen in the ^6LiH, or on protons in ^6Li in the same target, or on the ^6LiD target. This parameter depends on the beam polarization only. The relative normalization systematic error in P_B was ±3 %, and the error provided by the uncertainty in the p-C analyzing power was ±6 %.

TABLE 1

T_{kin} (GeV)	θ_{CM} (deg)	Points	Accelerator	Beam	Target	Ref.
A_{oono} and A_{ooon}						
1.00, 1.10	43–87	46	SATURNE II	p pol.	PPT	[11]
1.09–2.39	18–94	80	SATURNE II	p pol.	CH_2	[12]
1.10–2.40	18–98	212	SATURNE II	p pol.	PPT	[12]
1.97–2.49	70–110	87	SATURNE II	p pol.	CH_2	[13]
1.98–2.50	∼40	15	SATURNE II	p pol.	CH_2	[13]
2.16–2.28	19–52	126	SATURNE II	p	PPT	[14]
2.10–2.31	36–52	44	SATURNE II	p pol.	CH_2	[15]
1.15	59–89	15	SATURNE II	d pol.	PPT	[16]
1.80–2.50	58–110	740	SATURNE II	p pol.	PPT	[17]
1.00–1.15	42–82	50	SATURNE II	p pol.	CH_2	[18]
1.00–2.44	3–15	26	SATURNE II	p pol.	Scint.	[19]
1.74	9–108	11	SATURNE I	p	PPT	[20]
1.03, 1.19	14–87	46	SATURNE I	p	PPT	[21]
1.03–2.24	25–88	46	BNL COS.	p	PPT	[22]
1.70	23–37	6	LBL BEV.	p	PPT	[23]
1.04–1.96	23–88	71	CERN-PS	p	PPT	[24]
1.36	11–25	19	ITEP	p pol.	CH_2	[25]
1.03	9–87	6	ANL-ZGS	p pol.	LH_2	[26]
1.27, 2.21	18–119	39	ANL-ZGS	p pol.	PPT	[27]
1.73–2.44	26–97	94	ANL-ZGS	p	PPT	[28]
1.05–2.30	∼38	3	ANL-ZGS	p pol.	LH_2	[29]
1.05–1.97	32–92	37	ANL-ZGS	p pol.	PPT	[30]
1.27, 2.21	33–87	28	ANL-ZGS	p pol.	LD_2	[31]
1.27, 2.21	22–68	26	ANL-ZGS	p pol.	LD_2	[32]
1.00–2.00	∼ 34	64	KEK	p pol.	CH_2	[33]
A_{oonn}						
1.00–1.10	42–87	44	SATURNE II	p pol.	PPT	[11]
1.10–2.40	20–97	207	SATURNE II	p pol.	PPT	[34]
1.80–2.50	58–110	740	SATURNE II	p pol.	PPT	[17]
0.98, 1.19	14–87	25	SATURNE I	p scat.	PPT	[21]
1.27, 2.21	18–119	39	ANL-ZGS	p pol.	PPT	[27]
1.05–2.30	90	3	ANL-ZGS	p pol.	PPT	[29]
1.05–1.97	32–92	37	ANL-ZGS	p pol.	PPT	[30]

TABLE 2

		$T_{kin} = 1.095$ GeV,	$p_{lab} = 1.804$ GeV/c	
θ_{CM} (deg)	-t $(\mathrm{GeV/c})^2$	$A_{oono}(pp)$ H	$A_{oono}(pp)$ $^6Li + D\,(+H)$	$A_{oono}(pp)$ ^6Li
50.5	0.374	$+0.398 \pm 0.007$	$+0.413 \pm 0.009$	$+0.346 \pm 0.014$
52.0	0.395	$+0.372 \pm 0.004$	$+0.407 \pm 0.004$	$+0.362 \pm 0.006$
54.0	0.423	$+0.366 \pm 0.004$	$+0.380 \pm 0.003$	$+0.339 \pm 0.005$
56.0	0.453	$+0.360 \pm 0.004$	$+0.358 \pm 0.003$	$+0.320 \pm 0.005$
58.0	0.483	$+0.339 \pm 0.005$	$+0.342 \pm 0.003$	$+0.303 \pm 0.005$
60.0	0.514	$+0.321 \pm 0.004$	$+0.321 \pm 0.004$	$+0.280 \pm 0.005$
62.0	0.545	$+0.291 \pm 0.005$	$+0.303 \pm 0.004$	$+0.280 \pm 0.005$
64.0	0.577	$+0.277 \pm 0.005$	$+0.279 \pm 0.004$	$+0.256 \pm 0.006$
66.0	0.609	$+0.246 \pm 0.005$	$+0.250 \pm 0.004$	$+0.228 \pm 0.006$
68.0	0.625	$+0.212 \pm 0.005$	$+0.230 \pm 0.004$	$+0.217 \pm 0.006$
70.0	0.676	$+0.202 \pm 0.006$	$+0.213 \pm 0.004$	$+0.178 \pm 0.006$
72.0	0.710	$+0.177 \pm 0.006$	$+0.179 \pm 0.004$	$+0.167 \pm 0.007$
74.0	0.744	$+0.140 \pm 0.006$	$+0.164 \pm 0.004$	$+0.161 \pm 0.007$
76.0	0.779	$+0.121 \pm 0.006$	$+0.131 \pm 0.005$	$+0.128 \pm 0.007$
78.0	0.814	$+0.099 \pm 0.006$	$+0.117 \pm 0.005$	$+0.099 \pm 0.007$
80.0	0.849	$+0.075 \pm 0.006$	$+0.096 \pm 0.005$	$+0.098 \pm 0.007$
82.0	0.884	$+0.058 \pm 0.006$	$+0.071 \pm 0.005$	$+0.053 \pm 0.007$
84.0	0.920	$+0.037 \pm 0.007$	$+0.060 \pm 0.005$	$+0.046 \pm 0.007$
86.0	0.956	$+0.031 \pm 0.007$	$+0.031 \pm 0.005$	$+0.050 \pm 0.008$
88.0	0.991	-0.003 ± 0.007	$+0.015 \pm 0.005$	$+0.024 \pm 0.008$
90.0	1.027	-0.020 ± 0.007	$+0.013 \pm 0.006$	$+0.012 \pm 0.009$
91.5	1.054	-0.016 ± 0.010		
91.9	1.061		-0.022 ± 0.007	-0.014 ± 0.011
93.6	1.092		-0.032 ± 0.013	-0.030 ± 0.017

TABLE 2 – Continued

T_{kin} = 1.595 GeV,			p_{lab} = 2.353 GeV/c		
θ_{CM} (deg)	-t (GeV/c)^2	$A_{oono}(pp)$ $^6Li + D\ (+H)$	θ_{CM} (deg)	-t (GeV/c)^2	$A_{oono}(pp)$ $^6Li + D\ (+H)$
60.1	0.751	$+0.090 \pm 0.009$	82.0	1.288	-0.010 ± 0.008
62.0	0.795	$+0.062 \pm 0.007$	84.0	1.340	-0.002 ± 0.008
64.0	0.841	$+0.052 \pm 0.007$	86.0	1.392	$+0.005 \pm 0.008$
66.0	0.888	$+0.043 \pm 0.006$	88.0	1.444	$+0.013 \pm 0.008$
68.0	0.936	$+0.040 \pm 0.007$	90.0	1.497	-0.011 ± 0.008
70.0	0.984	$+0.019 \pm 0.007$	92.0	1.549	-0.004 ± 0.008
72.0	1.034	$+0.016 \pm 0.007$	94.0.	1.600	-0.004 ± 0.009
74.0	1.084	$+0.024 \pm 0.007$	95.9	1.652	$+0.000 \pm 0.010$
76.0	1.134	$+0.005 \pm 0.008$	97.9	1.702	$+0.014 \pm 0.012$
78.0	1.185	$+0.004 \pm 0.008$	99.8	1.751	-0.006 ± 0.019
80.0	1.237	$+0.021 \pm 0.008$	101.4	1.793	-0.057 ± 0.057

TABLE 2 - Continued

	T_{kin} = 1.795 GeV,		p_{lab} = 2.567 GeV/c	
θ_{CM} (deg)	-t $(GeV/c)^2$	$A_{oono}(pp)$ H	$A_{oono}(pp)$ $^6Li + D\,(+H)$	$A_{oono}(pp)$ ^6Li
61.3	0.876		$+0.040 \pm 0.018$	
63.2	0.925	$+0.105 \pm 0.043$	$+0.051 \pm 0.009$	$+0.092 \pm 0.045$
65.0	0.973	$+0.101 \pm 0.037$	$+0.065 \pm 0.009$	$+0.025 \pm 0.040$
67.0	1.025	$+0.068 \pm 0.029$	$+0.041 \pm 0.009$	$+0.089 \pm 0.039$
69.0	1.080	$+0.065 \pm 0.030$	$+0.050 \pm 0.009$	$+0.094 \pm 0.038$
71.0	1.136	$+0.094 \pm 0.030$	$+0.055 \pm 0.009$	$+0.051 \pm 0.040$
73.0	1.191	$+0.120 \pm 0.030$	$+0.056 \pm 0.009$	$+0.076 \pm 0.040$
75.0	1.248	$+0.013 \pm 0.033$	$+0.045 \pm 0.010$	$+0.029 \pm 0.041$
77.0	1.305	$+0.031 \pm 0.032$	$+0.060 \pm 0.010$	-0.042 ± 0.042
79.0	1.362	$+0.086 \pm 0.035$	$+0.038 \pm 0.010$	$+0.118 \pm 0.044$
81.0	1.421	-0.059 ± 0.035	$+0.042 \pm 0.011$	$+0.100 \pm 0.043$
83.0	1.480	$+0.014 \pm 0.034$	$+0.019 \pm 0.011$	$+0.037 \pm 0.045$
85.0	1.536	$+0.043 \pm 0.034$	$+0.022 \pm 0.010$	$+0.047 \pm 0.045$
87.0	1.596	-0.065 ± 0.032	-0.002 ± 0.010	$+0.001 \pm 0.043$
89.0	1.656	-0.005 ± 0.033	$+0.022 \pm 0.010$	-0.027 ± 0.045
91.0	1.713	$+0.000 \pm 0.035$	-0.007 ± 0.010	-0.041 ± 0.044
93.0	1.771	-0.014 ± 0.035	$+0.014 \pm 0.011$	-0.026 ± 0.046
95.1	1.833	$+0.004 \pm 0.036$	-0.023 ± 0.011	-0.074 ± 0.047
97.0	1.889	-0.051 ± 0.036	-0.024 ± 0.011	$+0.033 \pm 0.046$
99.0	1.949	-0.037 ± 0.035	-0.026 ± 0.011	-0.018 ± 0.047
100.8	1.999	$+0.023 \pm 0.039$	-0.031 ± 0.012	-0.045 ± 0.056
102.8	2.059		$+0.002 \pm 0.019$	-0.052 ± 0.067
104.7	2.111		-0.025 ± 0.033	

TABLE 2 – Continued

		$T_{kin} = 1.895$ GeV,	$p_{lab} = 2.674$ GeV/c	
θ_{CM} (deg)	-t $(\mathrm{GeV/c})^2$	$A_{oono}(pp)$ H	$A_{oono}(pp)$ $^6Li + D\,(+H)$	$A_{oono}(pp)$ ^6Li
61.5	0.930	$+0.080 \pm 0.049$	$+0.068 \pm 0.048$	$+0.060 \pm 0.040$
63.1	0.973	$+0.087 \pm 0.016$	$+0.017 \pm 0.028$	$+0.043 \pm 0.023$
65.0	1.027	$+0.097 \pm 0.016$	$+0.054 \pm 0.026$	$+0.076 \pm 0.021$
66.9	1.082	$+0.100 \pm 0.017$	$+0.105 \pm 0.025$	$+0.075 \pm 0.021$
69.0	1.142	$+0.071 \pm 0.017$	$+0.067 \pm 0.026$	$+0.113 \pm 0.021$
71.0	1.199	$+0.072 \pm 0.016$	$+0.072 \pm 0.026$	$+0.083 \pm 0.021$
73.0	1.258	$+0.086 \pm 0.016$	$+0.110 \pm 0.026$	$+0.063 \pm 0.022$
75.0	1.317	$+0.088 \pm 0.016$	$+0.044 \pm 0.026$	$+0.057 \pm 0.022$
77.0	1.378	$+0.077 \pm 0.017$	$+0.042 \pm 0.027$	$+0.105 \pm 0.023$
79.0	1.438	$+0.082 \pm 0.017$	$+0.061 \pm 0.028$	$+0.086 \pm 0.023$
81.0	1.500	$+0.032 \pm 0.018$	$+0.073 \pm 0.029$	$+0.055 \pm 0.024$
83.0	1.561	$+0.072 \pm 0.017$	-0.052 ± 0.028	$+0.017 \pm 0.024$
85.0	1.623	$+0.040 \pm 0.018$	$+0.053 \pm 0.028$	$+0.046 \pm 0.024$
87.0	1.685	$+0.000 \pm 0.017$	$+0.040 \pm 0.027$	$+0.000 \pm 0.023$
89.0	1.747	-0.020 ± 0.017	-0.023 ± 0.028	$+0.043 \pm 0.024$
91.0	1.809	-0.017 ± 0.017	-0.013 ± 0.029	-0.013 ± 0.024
93.0	1.871	-0.050 ± 0.019	$+0.000 \pm 0.029$	-0.024 ± 0.024
95.1	1.933	-0.045 ± 0.018	-0.030 ± 0.029	-0.042 ± 0.024
97.0	1.994	-0.046 ± 0.018	$+0.007 \pm 0.028$	-0.049 ± 0.024
99.0	2.056	-0.061 ± 0.018	-0.055 ± 0.029	-0.020 ± 0.025
101.0	2.117	-0.081 ± 0.018	-0.087 ± 0.031	-0.002 ± 0.027
102.3	2.157	-0.089 ± 0.044		
102.8	2.173		-0.112 ± 0.043	-0.051 ± 0.032
104.8	2.234		-0.146 ± 0.070	-0.073 ± 0.045

TABLE 2 – Continued

		$T_{kin} = 2.035$ GeV,	$p_{lab} = 2.822$ GeV/c	
θ_{CM} (deg)	-t $(\mathrm{GeV/c})^2$	$A_{oono}(pp)$ H	$A_{oono}(pp)$ $^6Li + D\,(+H)$	$A_{oono}(pp)$ ^6Li
61.4	0.995	$+0.129 \pm 0.026$	$+0.084 \pm 0.042$	$+0.078 \pm 0.043$
63.0	1.043	$+0.117 \pm 0.017$	$+0.100 \pm 0.026$	$+0.071 \pm 0.025$
65.0	1.102	$+0.159 \pm 0.018$	$+0.108 \pm 0.024$	$+0.097 \pm 0.021$
67.0	1.163	$+0.117 \pm 0.018$	$+0.109 \pm 0.024$	$+0.065 \pm 0.021$
69.0	1.226	$+0.102 \pm 0.019$	$+0.122 \pm 0.025$	$+0.106 \pm 0.021$
71.0	1.288	$+0.145 \pm 0.017$	$+0.055 \pm 0.025$	$+0.079 \pm 0.022$
73.0	1.351	$+0.107 \pm 0.018$	$+0.081 \pm 0.025$	$+0.129 \pm 0.022$
75.0	1.414	$+0.109 \pm 0.018$	$+0.123 \pm 0.026$	$+0.095 \pm 0.023$
77.0	1.480	$+0.107 \pm 0.018$	$+0.084 \pm 0.027$	$+0.104 \pm 0.024$
79.0	1.544	$+0.085 \pm 0.019$	$+0.119 \pm 0.026$	$+0.037 \pm 0.024$
81.0	1.610	$+0.075 \pm 0.020$	$+0.062 \pm 0.028$	$+0.063 \pm 0.024$
83.0	1.677	$+0.074 \pm 0.019$	$+0.068 \pm 0.027$	$+0.070 \pm 0.024$
85.0	1.744	$+0.022 \pm 0.019$	$+0.044 \pm 0.027$	$+0.033 \pm 0.025$
87.0	1.810	$+0.033 \pm 0.019$	$+0.069 \pm 0.027$	$+0.030 \pm 0.024$
89.0	1.876	-0.002 ± 0.019	$+0.031 \pm 0.028$	$+0.022 \pm 0.024$
91.0	1.943	$+0.020 \pm 0.019$	-0.037 ± 0.027	-0.008 ± 0.025
93.0	2.009	-0.031 ± 0.020	$+0.010 \pm 0.028$	$+0.015 \pm 0.025$
95.0	2.076	-0.044 ± 0.020	-0.045 ± 0.028	-0.041 ± 0.025
97.0	2.144	-0.039 ± 0.020	-0.080 ± 0.028	-0.060 ± 0.025
99.0	2.208	-0.068 ± 0.020	-0.081 ± 0.028	-0.070 ± 0.025
101.0	2.274	-0.080 ± 0.020	-0.086 ± 0.029	-0.029 ± 0.026
102.8	2.332	-0.119 ± 0.023	-0.019 ± 0.032	-0.063 ± 0.030
104.9	2.399		-0.033 ± 0.049	-0.070 ± 0.035

TABLE 2 – Continued

		T_{kin} = 2.095 GeV,	p_{lab} = 2.885 GeV/c	
θ_{CM} (deg)	-t $(\mathrm{GeV/c})^2$	$A_{oono}(pp)$ H	$A_{oono}(pp)$ $^6Li + D\ (+H)$	$A_{oono}(pp)$ ^6Li
61.1	1.021	$+0.175 \pm 0.026$	$+0.108 \pm 0.022$	
63.0	1.074	$+0.167 \pm 0.021$	$+0.140 \pm 0.014$	$+0.175 \pm 0.029$
65.0	1.135	$+0.193 \pm 0.021$	$+0.152 \pm 0.013$	$+0.121 \pm 0.025$
67.0	1.197	$+0.155 \pm 0.021$	$+0.126 \pm 0.013$	$+0.109 \pm 0.025$
69.0	1.260	$+0.109 \pm 0.023$	$+0.125 \pm 0.013$	$+0.101 \pm 0.025$
71.0	1.326	$+0.136 \pm 0.021$	$+0.146 \pm 0.013$	$+0.081 \pm 0.026$
73.0	1.391	$+0.149 \pm 0.021$	$+0.119 \pm 0.013$	$+0.139 \pm 0.026$
75.0	1.457	$+0.131 \pm 0.022$	$+0.098 \pm 0.014$	$+0.103 \pm 0.027$
77.0	1.523	$+0.130 \pm 0.021$	$+0.109 \pm 0.014$	$+0.140 \pm 0.028$
79.0	1.590	$+0.099 \pm 0.022$	$+0.124 \pm 0.014$	$+0.094 \pm 0.029$
81.0	1.657	$+0.116 \pm 0.023$	$+0.089 \pm 0.014$	$+0.051 \pm 0.030$
83.0	1.727	$+0.133 \pm 0.025$	$+0.077 \pm 0.015$	$+0.078 \pm 0.030$
85.0	1.795	$+0.024 \pm 0.024$	$+0.043 \pm 0.014$	$+0.050 \pm 0.031$
87.0	1.863	$+0.034 \pm 0.024$	$+0.053 \pm 0.014$	$+0.081 \pm 0.031$
89.0	1.931	$+0.008 \pm 0.024$	$+0.018 \pm 0.015$	$+0.015 \pm 0.031$
91.0	2.000	-0.040 ± 0.025	-0.019 ± 0.014	$+0.010 \pm 0.031$
93.0	2.068	-0.086 ± 0.025	-0.045 ± 0.015	-0.027 ± 0.032
95.0	2.137	-0.046 ± 0.027	-0.053 ± 0.015	-0.066 ± 0.031
97.0	2.206	-0.092 ± 0.026	-0.057 ± 0.015	-0.034 ± 0.032
99.0	2.273	-0.122 ± 0.025	-0.121 ± 0.015	-0.127 ± 0.032
101.0	2.341	-0.086 ± 0.026	-0.087 ± 0.015	-0.053 ± 0.033
102.9	2.406	-0.068 ± 0.027	-0.105 ± 0.017	-0.082 ± 0.036

TABLE 2 – Continued

		$T_{kin} = 2.395$ GeV,	$p_{lab} = 3.199$ GeV/c	
θ_{CM} (deg)	-t (GeV/c)^2	$A_{oono}(pp)$ H	$A_{oono}(pp)$ $^6Li + D\ (+H)$	$A_{oono}(pp)$ ^6Li
61.7	1.181	$+0.186 \pm 0.031$	$+0.191 \pm 0.057$	$+0.185 \pm 0.046$
63.0	1.226	$+0.225 \pm 0.015$	$+0.185 \pm 0.032$	$+0.208 \pm 0.025$
65.0	1.297	$+0.253 \pm 0.015$	$+0.214 \pm 0.028$	$+0.203 \pm 0.020$
67.0	1.369	$+0.200 \pm 0.016$	$+0.174 \pm 0.028$	$+0.179 \pm 0.019$
69.0	1.442	$+0.232 \pm 0.016$	$+0.171 \pm 0.029$	$+0.170 \pm 0.020$
70.9	1.513	$+0.211 \pm 0.017$	$+0.209 \pm 0.029$	$+0.126 \pm 0.020$
73.0	1.590	$+0.208 \pm 0.017$	$+0.179 \pm 0.030$	$+0.183 \pm 0.021$
75.0	1.666	$+0.194 \pm 0.016$	$+0.170 \pm 0.030$	$+0.177 \pm 0.022$
77.0	1.741	$+0.174 \pm 0.017$	$+0.180 \pm 0.031$	$+0.126 \pm 0.022$
79.0	1.818	$+0.146 \pm 0.018$	$+0.105 \pm 0.031$	$+0.121 \pm 0.022$
81.0	1.895	$+0.099 \pm 0.018$	$+0.109 \pm 0.032$	$+0.098 \pm 0.023$
83.0	1.973	$+0.070 \pm 0.018$	$+0.078 \pm 0.033$	$+0.085 \pm 0.023$
85.0	2.052	$+0.057 \pm 0.018$	$+0.071 \pm 0.033$	$+0.039 \pm 0.024$
87.0	2.129	$+0.014 \pm 0.018$	$+0.087 \pm 0.034$	$+0.011 \pm 0.024$
89.0	2.207	-0.013 ± 0.019	$+0.004 \pm 0.034$	-0.019 ± 0.024
91.0	2.287	-0.008 ± 0.019	-0.006 ± 0.034	-0.038 ± 0.024
93.0	2.365	-0.043 ± 0.019	-0.034 ± 0.034	-0.059 ± 0.024
95.0	2.443	-0.086 ± 0.019	-0.154 ± 0.034	-0.062 ± 0.023
97.0	2.521	-0.149 ± 0.019	-0.113 ± 0.033	-0.099 ± 0.023
99.0	2.599	-0.141 ± 0.019	-0.122 ± 0.033	-0.077 ± 0.023
101.0	2.676	-0.174 ± 0.018	-0.158 ± 0.033	-0.147 ± 0.023
103.0	2.753	-0.171 ± 0.018	-0.130 ± 0.033	-0.156 ± 0.024
105.0	2.828	-0.206 ± 0.018	-0.123 ± 0.040	-0.164 ± 0.033

TABLE 3

$T_{kin} = 1.091$ GeV, $p_{lab} = 1.800$ GeV/c

θ_{CM} (deg)	-t $(\mathrm{GeV/c})^2$	$A_{oono}(pp)$ H	$A_{oono}(pp)$ C
61.3	0.532	$+0.310 \pm 0.009$	$+0.262 \pm 0.016$
63.1	0.561	$+0.291 \pm 0.005$	$+0.227 \pm 0.012$
65.0	0.591	$+0.262 \pm 0.005$	$+0.204 \pm 0.012$
67.0	0.624	$+0.247 \pm 0.005$	$+0.205 \pm 0.011$
69.0	0.657	$+0.208 \pm 0.005$	$+0.197 \pm 0.012$
70.9	0.689	$+0.192 \pm 0.006$	$+0.195 \pm 0.013$
73.0	0.725	$+0.144 \pm 0.006$	$+0.174 \pm 0.014$
75.0	0.759	$+0.141 \pm 0.007$	$+0.119 \pm 0.015$
77.0	0.794	$+0.121 \pm 0.008$	$+0.132 \pm 0.017$
79.0	0.829	$+0.096 \pm 0.008$	$+0.082 \pm 0.019$
81.0	0.864	$+0.075 \pm 0.010$	$+0.076 \pm 0.021$
83.0	0.899	$+0.040 \pm 0.011$	$+0.063 \pm 0.024$
85.0	0.935	$+0.058 \pm 0.013$	$+0.018 \pm 0.027$
87.0	0.970	$+0.031 \pm 0.016$	$+0.071 \pm 0.033$
89.0	1.006	-0.011 ± 0.019	$+0.049 \pm 0.044$
90.8	1.038	-0.026 ± 0.026	$+0.051 \pm 0.072$
$T_{kin} = 1.592$ GeV,		$p_{lab} = 2.350$ GeV/c	
71.0	1.007	$+0.001 \pm 0.037$	
76.9	1.155	-0.004 ± 0.021	$+0.061 \pm 0.035$
84.9	1.361	$+0.021 \pm 0.022$	$+0.019 \pm 0.036$
92.9	1.569	$+0.033 \pm 0.024$	$+0.013 \pm 0.038$
98.5	1.714	-0.083 ± 0.040	
$T_{kin} = 1.792$ GeV,		$p_{lab} = 2.564$ GeV/c	
75.4	1.258	$+0.047 \pm 0.036$	$+0.059 \pm 0.062$
79.0	1.361	$+0.055 \pm 0.026$	-0.025 ± 0.045
83.0	1.476	-0.006 ± 0.028	$+0.119 \pm 0.044$
87.0	1.593	-0.057 ± 0.029	-0.087 ± 0.044
91.0	1.711	$+0.003 \pm 0.029$	
92.8	1.763		-0.051 ± 0.031
95.0	1.828	-0.023 ± 0.030	
99.0	1.944	-0.051 ± 0.030	
99.4	1.956		-0.003 ± 0.042
101.9	2.028	$+0.009 \pm 0.045$	

TABLE 3 - Continued

θ_{CM} (deg)	-t $(\mathrm{GeV/c})^2$	$A_{oono}(pp)$ H	$A_{oono}(pp)$ C
$T_{kin} = 1.892$ GeV,		$p_{lab} = 2.670$ GeV/c	
75.4	1.328	$+0.139 \pm 0.053$	$+0.116 \pm 0.095$
79.0	1.436	$+0.087 \pm 0.035$	-0.020 ± 0.065
83.0	1.559	-0.001 ± 0.038	$+0.033 \pm 0.059$
86.9	1.679	$+0.042 \pm 0.038$	$+0.116 \pm 0.057$
91.0	1.806	$+0.019 \pm 0.038$	$+0.069 \pm 0.057$
95.0	1.930	-0.032 ± 0.039	-0.007 ± 0.057
99.0	2.053	-0.051 ± 0.039	-0.109 ± 0.062
101.9	2.141		-0.122 ± 0.148
102.3	2.153	-0.106 ± 0.050	-0.122 ± 0.148
$T_{kin} = 2.032$ GeV,		$p_{lab} = 2.822$ GeV/c	
77.8	1.504	$+0.103 \pm 0.039$	$+0.096 \pm 0.097$
85.0	1.740	$+0.036 \pm 0.035$	$+0.077 \pm 0.053$
92.9	2.003	-0.074 ± 0.037	-0.010 ± 0.053
99.8	2.231	-0.028 ± 0.045	-0.074 ± 0.079
$T_{kin} = 2.092$ GeV,		$p_{lab} = 2.881$ GeV/c	
78.2	1.561	$+0.091 \pm 0.028$	$+0.111 \pm 0.045$
85.0	1.792	-0.014 ± 0.024	$+0.015 \pm 0.034$
93.0	2.066	-0.037 ± 0.026	-0.041 ± 0.035
99.5	2.287	-0.080 ± 0.032	-0.171 ± 0.051
$T_{kin} = 2.392$ GeV,		$p_{lab} = 3.195$ GeV/c	
78.4	1.793		$+0.122 \pm 0.064$
79.1	1.820	$+0.161 \pm 0.049$	
84.9	2.045	$+0.016 \pm 0.028$	
85.2	2.057		$+0.027 \pm 0.038$
93.1	2.366	-0.112 ± 0.028	-0.065 ± 0.038
98.5	2.576	-0.178 ± 0.045	
99.3	2.607		-0.025 ± 0.067

TABLE 4

	T_{kin} = 1.095 GeV,		p_{lab} = 1.804 GeV/c		
θ_{CM} (deg)	-t $(\mathrm{GeV/c})^2$	$A_{oonn}(pp)$ H	θ_{CM} (deg)	-t $(\mathrm{GeV/c})^2$	$A_{oonn}(pp)$ H
50.5	0.374	$+0.545 \pm 0.025$	72.0	0.710	$+0.518 \pm 0.019$
52.0	0.395	$+0.547 \pm 0.012$	74.0	0.744	$+0.527 \pm 0.019$
54.0	0.423	$+0.535 \pm 0.013$	76.0	0.779	$+0.532 \pm 0.019$
56.0	0.453	$+0.536 \pm 0.014$	78.0	0.814	$+0.509 \pm 0.020$
58.0	0.483	$+0.543 \pm 0.015$	80.0	0.849	$+0.549 \pm 0.020$
60.0	0.514	$+0.520 \pm 0.015$	82.0	0.884	$+0.518 \pm 0.022$
62.0	0.545	$+0.523 \pm 0.015$	84.0.	0.920	$+0.531 \pm 0.022$
64.0	0.577	$+0.544 \pm 0.016$	86.0	0.956	$+0.493 \pm 0.022$
66.0	0.609	$+0.525 \pm 0.017$	88.0	0.991	$+0.608 \pm 0.022$
68.0	0.625	$+0.514 \pm 0.017$	90.0	1.027	$+0.536 \pm 0.023$
70.0	0.676	$+0.526 \pm 0.019$	91.5	1.055	$+0.489 \pm 0.033$
θ_{CM} (deg)	-t $(\mathrm{GeV/c})^2$	$A_{oonn}(pp)$ $^6Li + D\ (+H)$	θ_{CM} (deg)	-t $(\mathrm{GeV/c})^2$	$A_{oonn}(pp)$ $^6Li + D\ (+H)$
53.3	0.413	$+0.525 \pm 0.031$	73.0	0.726	$+0.480 \pm 0.039$
57.0	0.467	$+0.557 \pm 0.030$	77.0	0.796	$+0.469 \pm 0.040$
61.0	0.529	$+0.529 \pm 0.031$	81.0	0.866	$+0.528 \pm 0.042$
64.9	0.592	$+0.480 \pm 0.033$	85.0	0.937	$+0.516 \pm 0.044$
68.9	0.658	$+0.476 \pm 0.037$	88.8	1.006	$+0.565 \pm 0.048$

	T_{kin} = 1.595 GeV,		p_{lab} = 2.353 GeV/c		
θ_{CM} (deg)	-t $(\mathrm{GeV/c})^2$	$A_{oonn}(pp)$ $^6Li + D\ (+H)$	θ_{CM} (deg)	-t $(\mathrm{GeV/c})^2$	$A_{oonn}(pp)$ $^6Li + D\ (+H)$
61.3	0.778	$+0.471 \pm 0.054$	81.0	1.236	$+0.465 \pm 0.053$
65.0	0.865	$+0.386 \pm 0.043$	85.0	1.340	$+0.465 \pm 0.053$
69.0	0.960	$+0.387 \pm 0.043$	89.0	1.444	$+0.555 \pm 0.053$
72.9	1.058	$+0.422 \pm 0.046$	92.9	1.548	$+0.608 \pm 0.054$
77.0	1.159	$+0.421 \pm 0.051$	96.7	1.648	$+0.458 \pm 0.068$

TABLE 5

T_{kin} = 1.095 GeV

p_{lab} = 1.804 GeV/c

θ_{CM} (deg)	Interval (CM deg)	$-t$ (mean) $(\mathrm{GeV/c})^2$	$D_{onon}(pp)$ H
55.3	51.0–59.0	0.443	0.642 ± 0.079
62.6	59.0–66.0	0.554	0.694 ± 0.087
70.3	66.0–75.0	0.681	0.884 ± 0.101
83.2	75.0–92.0	0.906	0.904 ± 0.097

TABLE 6

T_{kin} = 1.095 GeV, p_{lab} = 1.804 GeV/c					
θ_{CM} (deg)	Interval (CM deg)	−t (mean) $(\mathrm{GeV/c})^2$	$K_{onno}(pp)$ H	$K_{onno}(pp)$ $^6Li + D\,(+H)$	$K_{onno}(pp)$ ^6Li
54.0	49.5–56.0	0.425	0.668 ± 0.035	0.635 ± 0.032	0.558 ± 0.049
57.4	56.0–59.0	0.474	0.727 ± 0.041	0.693 ± 0.036	0.635 ± 0.052
61.0	59.0–63.0	0.529	0.817 ± 0.036	0.802 ± 0.032	0.738 ± 0.048
64.5	63.0–66.0	0.585	0.854 ± 0.041	0.843 ± 0.036	0.741 ± 0.058
68.0	66.0–70.0	0.643	0.809 ± 0.040	0.845 ± 0.035	0.727 ± 0.057
72.5	70.0–75.0	0.718	0.720 ± 0.043	0.794 ± 0.036	0.667 ± 0.060
78.4	75.0–82.0	0.821	0.781 ± 0.042	0.736 ± 0.037	0.752 ± 0.060
86.9	82.0–94.6	0.972	0.665 ± 0.044	0.684 ± 0.040	0.641 ± 0.063
T_{kin} = 1.595 GeV, p_{lab} = 2.353 GeV/c					
63.6	57.4–66.0	0.831		0.427 ± 0.066	
68.1	66.0–70.0	0.938		0.460 ± 0.069	
72.5	70.0–75.0	1.047		0.386 ± 0.069	
77.9	75.0–81.0	1.183		0.458 ± 0.075	
84.0	81.0–87.0	1.340		0.649 ± 0.081	
90.0	87.0–93.0	1.497		0.515 ± 0.081	
96.0	93.0–102.1	1.653		0.478 ± 0.090	
T_{kin} = 1.795 GeV, p_{lab} = 2.567 GeV/c					
67.4	60.7–71.0	1.037		0.228 ± 0.093	
75.5	71.0–80.0	1.262		0.517 ± 0.092	
85.1	80.7–90.0	1.540		0.461 ± 0.093	
96.1	90.0–105.9	1.863		0.466 ± 0.089	
T_{kin} = 1.895 GeV, p_{lab} = 2.674 GeV/c					
68.6	61.8–73.0	1.129	0.110 ± 0.148	0.009 ± 0.251	0.143 ± 0.193
79.0	73.0–85.0	1.439	0.207 ± 0.140	0.277 ± 0.241	0.268 ± 0.206
93.4	85.0–104.0	1.883	0.467 ± 0.125	0.635 ± 0.215	0.669 ± 0.183
T_{kin} = 2.035 GeV, p_{lab} = 2.822 GeV/c					
68.0	60.5–73.0	1.194	0.333 ± 0.148	0.224 ± 0.234	0.376 ± 0.204
78.9	73.0–85.0	1.542	0.272 ± 0.143	0.619 ± 0.224	0.529 ± 0.218
94.0	85.0–104.6	2.043	0.539 ± 0.136	0.549 ± 0.213	0.696 ± 0.195

TABLE 6 – Continued

T_{kin} = 2.095 GeV, $p_{\ell ab}$ = 2.885 GeV/c					
θ_{CM} (deg)	Interval (CM deg)	–t (mean) $(\mathrm{GeV/c})^2$	$K_{onno}(pp)$ H	$K_{onno}(pp)$ $^6Li + D\,(+H)$	$K_{onno}(pp)$ ^6Li
67.0	60.5–73.0	1.198	0.324 ± 0.181	0.227 ± 0.123	0.323 ± 0.244
78.3	73.0–84.0	1.567	0.099 ± 0.184	0.220 ± 0.126	0.525 ± 0.255
93.5	84.0–104.3	2.086	0.423 ± 0.172	0.370 ± 0.113	0.461 ± 0.247
T_{kin} = 2.395 GeV, $p_{\ell ab}$ = 3.199 GeV/c					
69.0	60.9–77.0	1.442	0.574 ± 0.120	$+0.000 \pm 0.243$	0.365 ± 0.166
90.7	77.0–106.2	2.275	0.582 ± 0.125	0.583 ± 0.237	0.392 ± 0.168

FIGURE CAPTIONS

Fig. 1 The normalized $\Delta\theta_{CM}$ distributions of pp events from ^6LiH and from ^6LiD targets at 1.095 GeV. The small peak in the ^6LiD distribution is due to the residual hydrogen. The solid curve was obtained by the Monte Carlo (MC) simulation for quasi-elastic and inelastic events in ^6LiH.

Fig. 2 $A_{oono}(pp)$ energy dependence at 1.095 GeV. The meaning of the symbols is: • ... protons scattered on H in the ^6LiH target, ▽ ...protons on $^6Li + D$ $(+H)$ in the ^6LiD target, △ ... protons on ^6Li, ○ ... [11], + ... [12], solid curve ... VPI-PSA, dashed curve ... SG-PSA.

Fig. 3 $A_{oono}(pp)$ energy dependence at 1.595 and 1.795 GeV. The meaning of the symbols is:

• ... protons scattered on H in the ^6LiH target, ▽ ...protons on ^6Li+D $(+H)$ in the ^6LiD target, ○ ... [12], solid curves ... VPI-PSA, dashed curves ... SG-PSA.

Fig. 4 $A_{oono}(pp)$ energy dependence at 1.895 and 2.035 GeV. The meaning of the symbols is:

• ... protons scattered on H in the ^6LiH target, ▽ ...protons on $^6Li + D$ $(+H)$ in the ^6LiD target, ○ ... final data at 1.935 GeV from [17], open square ... [13], solid curves ... VPI-PSA.

Fig. 5 $A_{oono}(pp)$ energy dependence at 2.095 and 2.395 GeV. The meaning of the symbols is:

• ... protons scattered on H in the ^6LiH target, ▽ ...protons on $^6Li + D$ $(+H)$ in the ^6LiD target, ○ ... [12], open square ... [13], ⋆ ... [15], × ... 2.44 GeV [19], solid curves ... VPI-PSA, dashed curves ... SG-PSA.

Fig. 6 CH_2 target results at 1.091 GeV. The meaning of the symbols is:
○ ... scattering of protons on H in the CH_2 target, • ... pp scattering on protons in C, solid curve ... VPI-PSA, dashed curve ... SG-PSA.

Fig. 7 $A_{oono}(pp)$ energy dependence at three energies. The curves are SG-PSA fits at 1.0, 1.1, and 1.3 GeV. The meaning of the symbols is: × ... 1.03 GeV ANL [26], △ ... 1.181 GeV CERN [24], + ... 1.194 GeV Saturne I [21], ○ ... Saturne II 1.295 GeV [12].

Fig. 8 $A_{oonn}(pp)$ energy dependence at 1.095 and 1.595 GeV. The meaning of the symbols is:

• ... protons scattered on H in the ^6LiH target, ▽ ...protons on ^6Li+D $(+H)$ in the ^6LiD target, + ...[11], ○ ... [34], × ... [30], solid curves ... VPI-PSA, dashed curves ... SG-PSA.

Fig. 9 $D_{onon}(\theta_{CM}) = K_{onno}(180° - \theta_{CM})$ energy dependence at 1.095, 1.595, 1.795, 1.895, 2.035, and 2.095 GeV. The meaning of the symbols is: • ... protons scattered on H in the ^6LiH target (K_{onno}), ▽ ...protons on $^6Li + D$ $(+H)$ in the ^6LiD target (K_{onno}), open squares ... D_{onon} measured with the ^6LiH target, ○ ... [36-38], + ... [9,39], ⋆ ... BNL 1.90 GeV [40], × ... 2.205 GeV ANL [41], solid curves ... VPI-PSA, dashed curves ... SG-PSA.

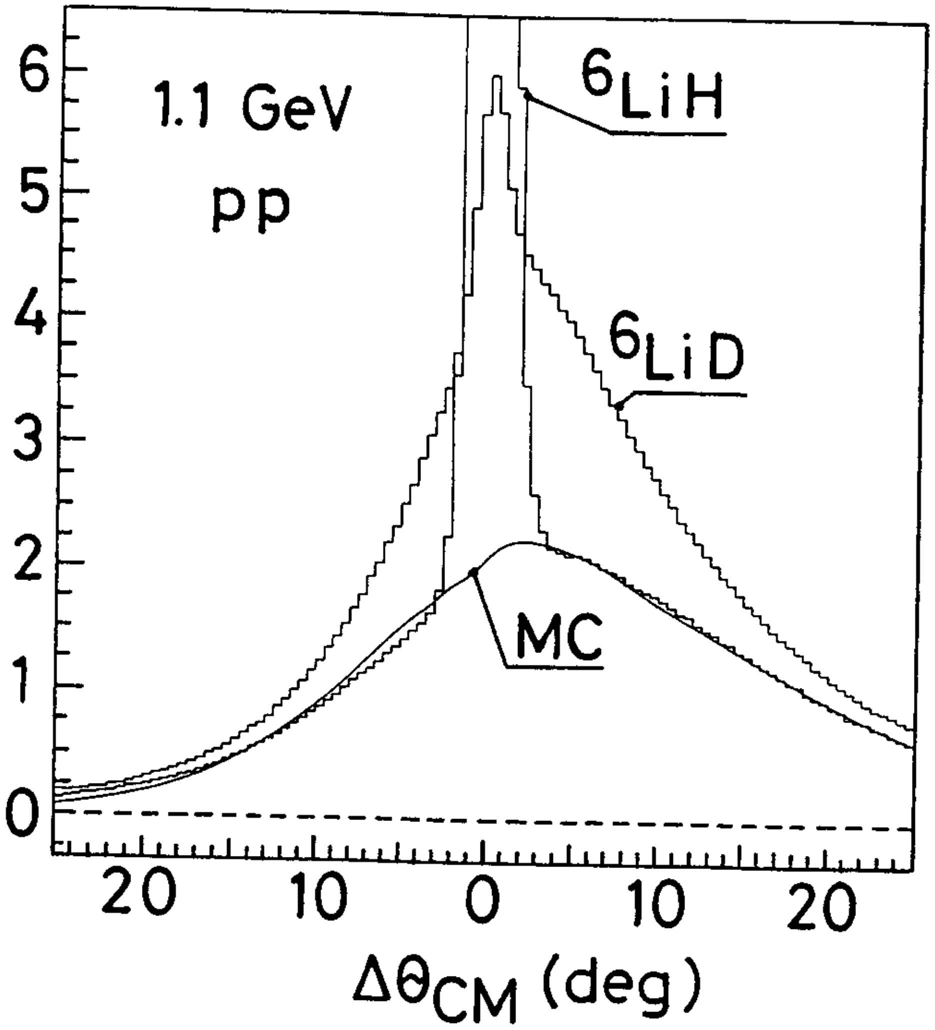

FIG. 1

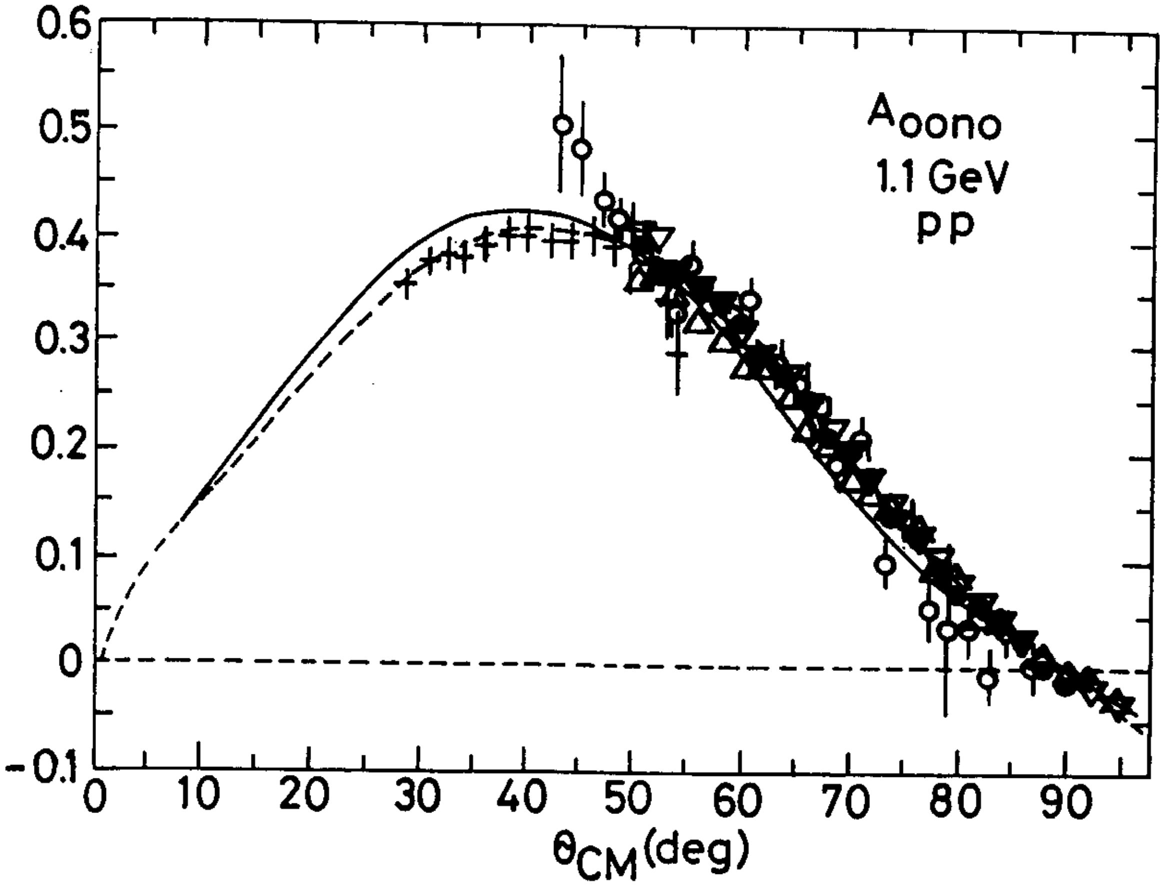
0.6
0.5
0.4
0.3
0.2
0.1
0
-0.1
0
10
20
30
40
50
60
70
80
90
θ_{CM}(deg)
A_{oono}
1.1 GeV
pp

FIG. 2

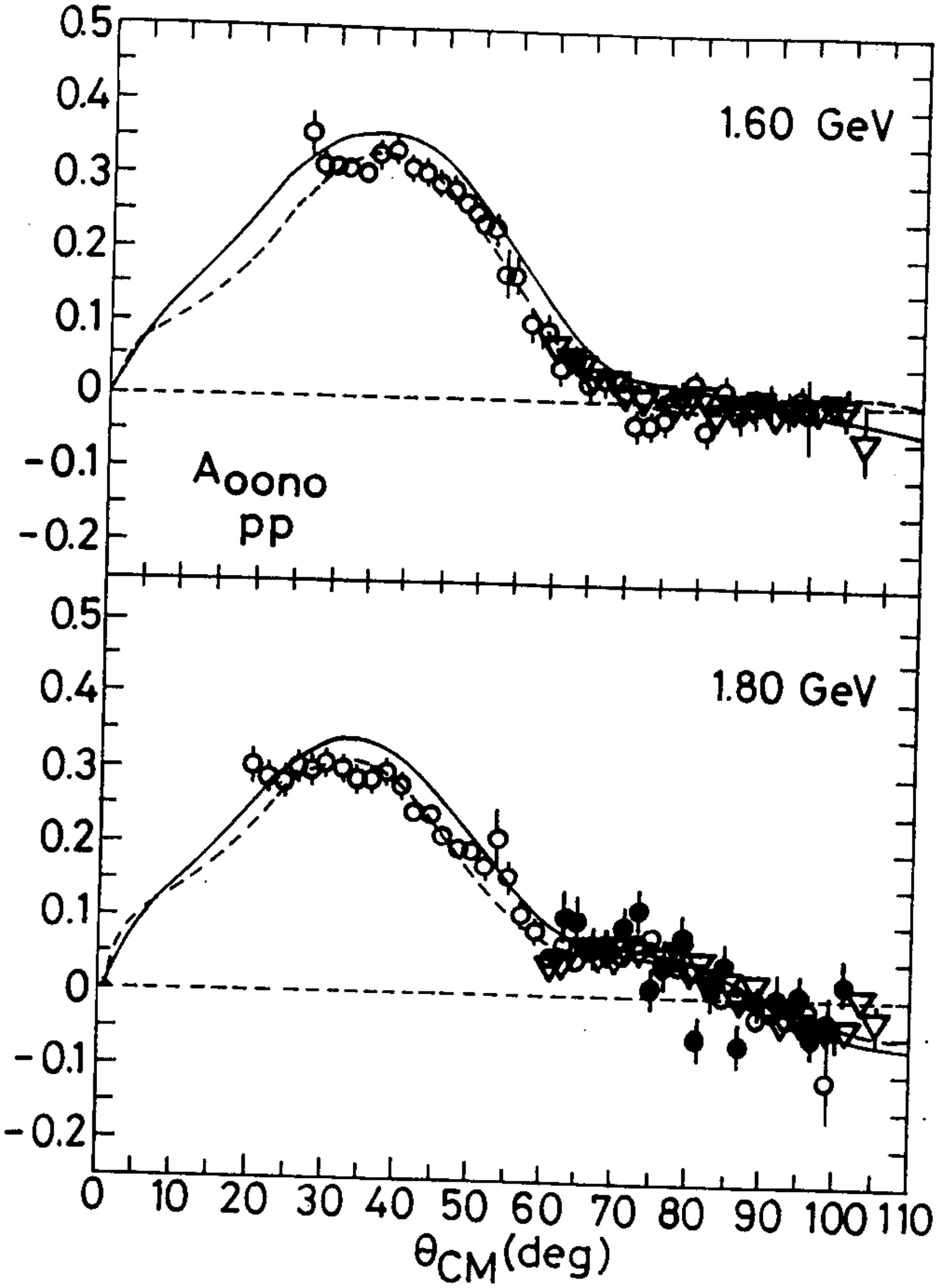
0.5
0.4
0.3
0.2
0.1
0
-0.1
-0.2
1.60 GeV
A_{oono}
pp
1.80 GeV
0
10
20
30
40
50
60
70
80
90
100
110
θ_{CM}(deg)

FIG. 3

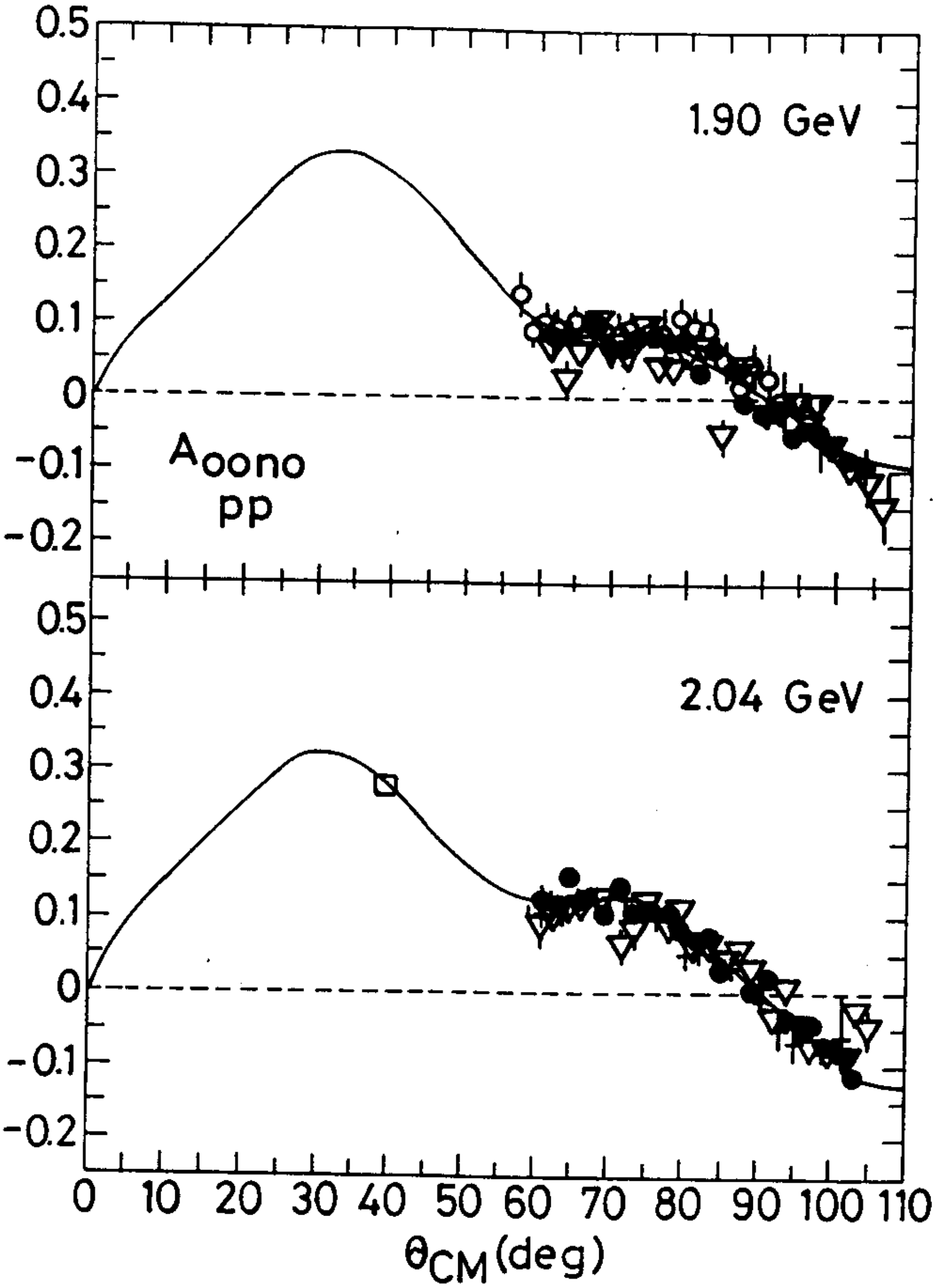
0.5
0.4
0.3
0.2
0.1
0
-0.1
-0.2
1.90 GeV
2.04 GeV
A_{oono}
pp
0
10
20
30
40
50
60
70
80
90
100
110
θ_{CM} (deg)

FIG. 4

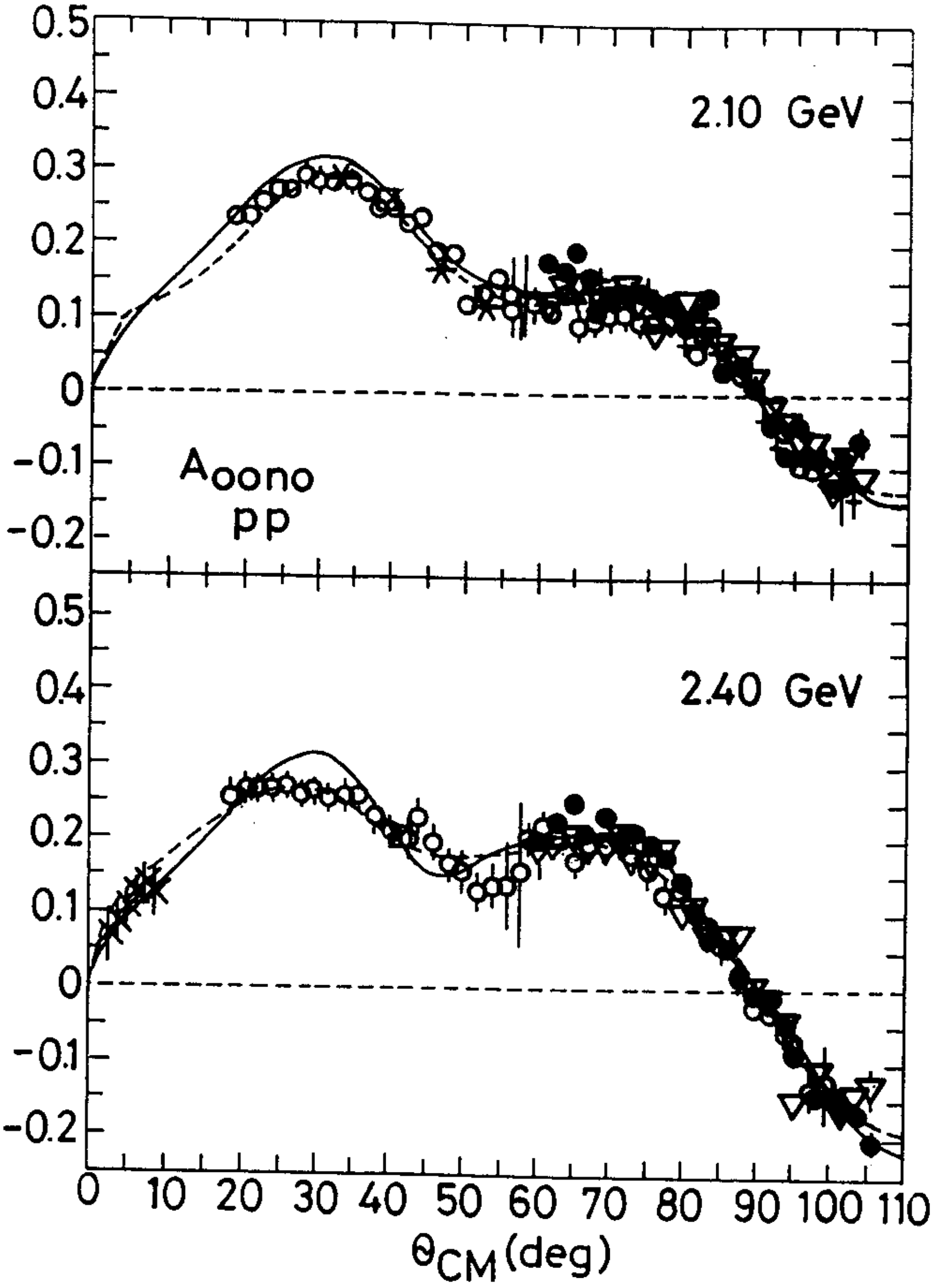
0.5
0.4
0.3
0.2
0.1
0
-0.1
-0.2
2.10 GeV
2.40 GeV
A_{oono}
pp
0
10
20
30
40
50
60
70
80
90
100
110
θ_{CM}(deg)

FIG. 5

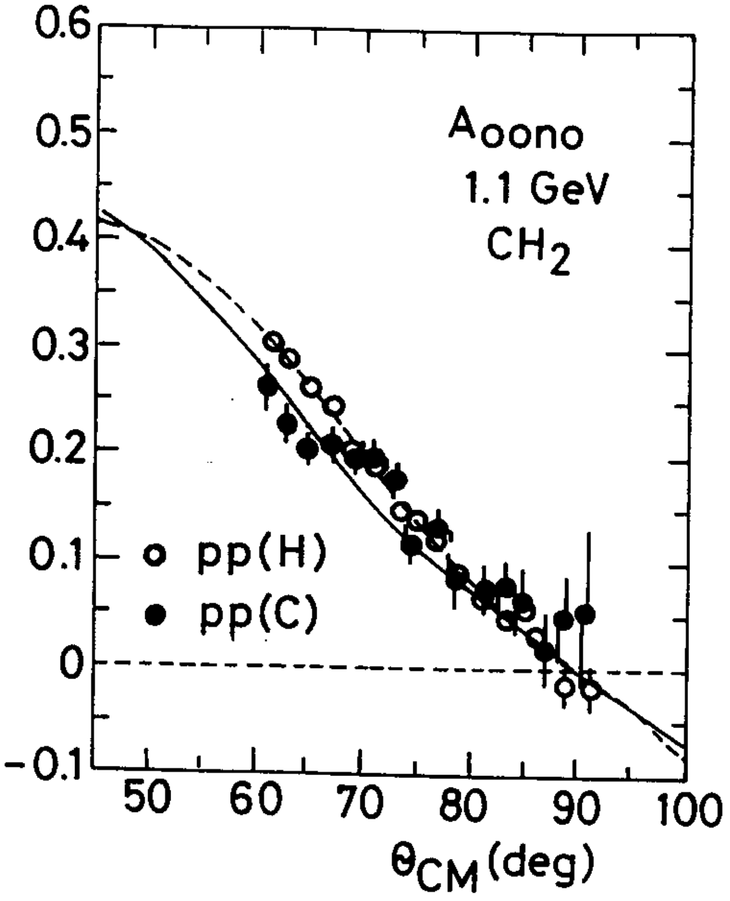
0.6
0.5
0.4
0.3
0.2
0.1
0
-0.1
50
60
70
80
90
100
θ_{CM} (deg)
A_{oono}
1.1 GeV
CH_2
○ pp(H)
● pp(C)

FIG. 6

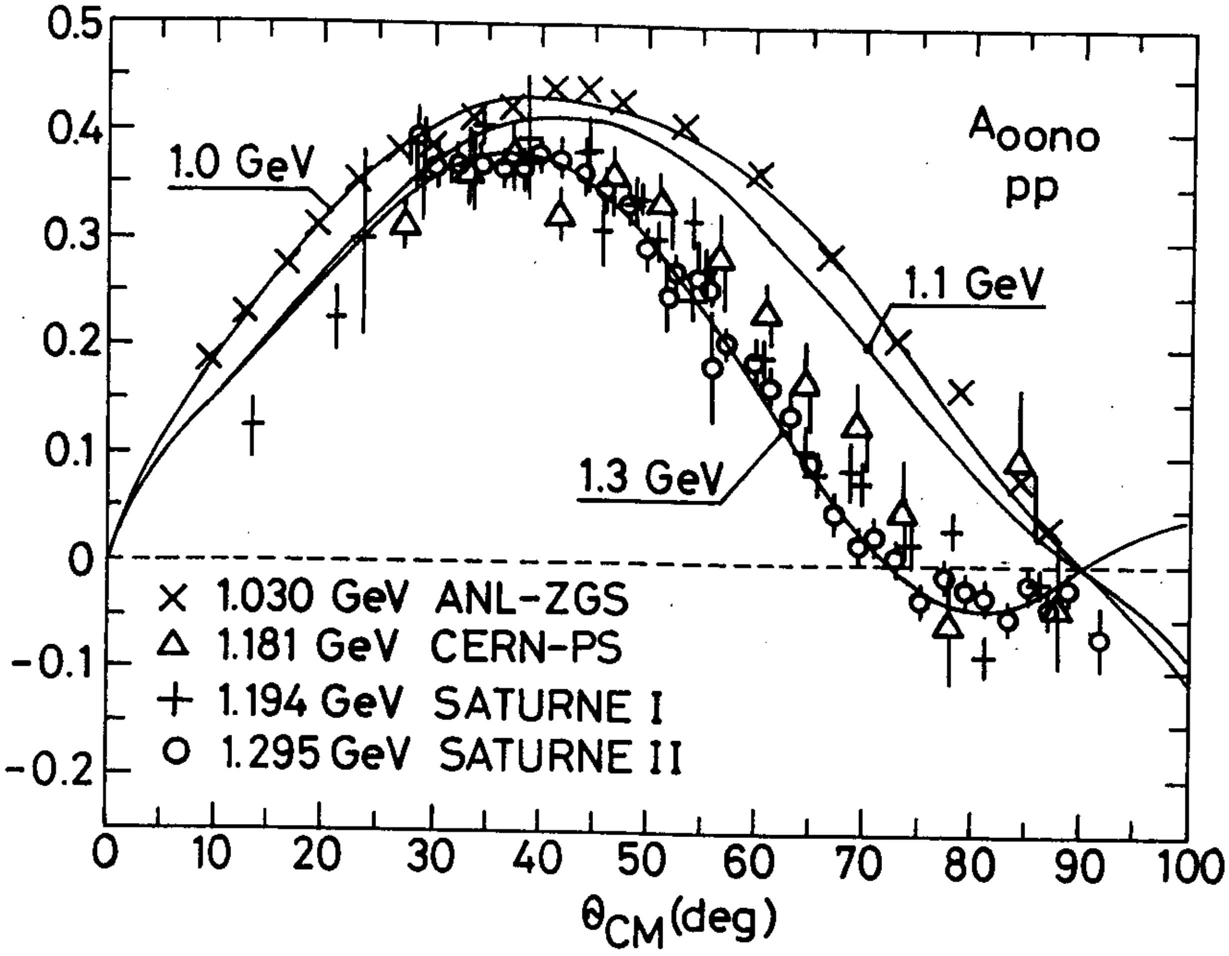

A_oono pp
1.0 GeV
1.1 GeV
1.3 GeV
× 1.030 GeV ANL-ZGS
△ 1.181 GeV CERN-PS
+ 1.194 GeV SATURNE I
○ 1.295 GeV SATURNE II
0.5
0.4
0.3
0.2
0.1
0
-0.1
-0.2
0
10
20
30
40
50
60
70
80
90
100
θ_CM (deg)

FIG. 7

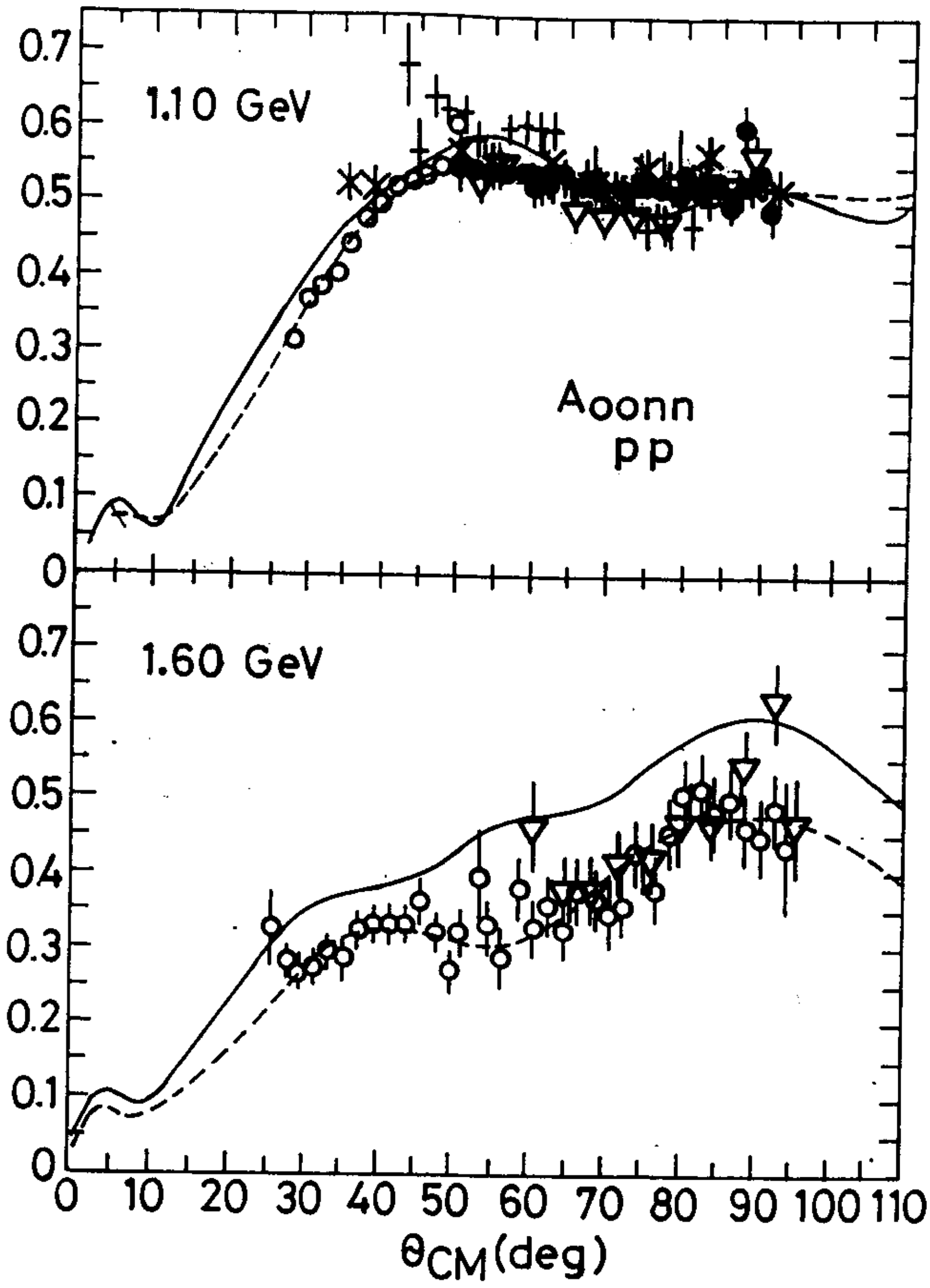
0.7
0.6
0.5
0.4
0.3
0.2
0.1
0
1.10 GeV
1.60 GeV
Aoonn
pp
0
10
20
30
40
50
60
70
80
90
100
110
θCM(deg)

FIG. 8

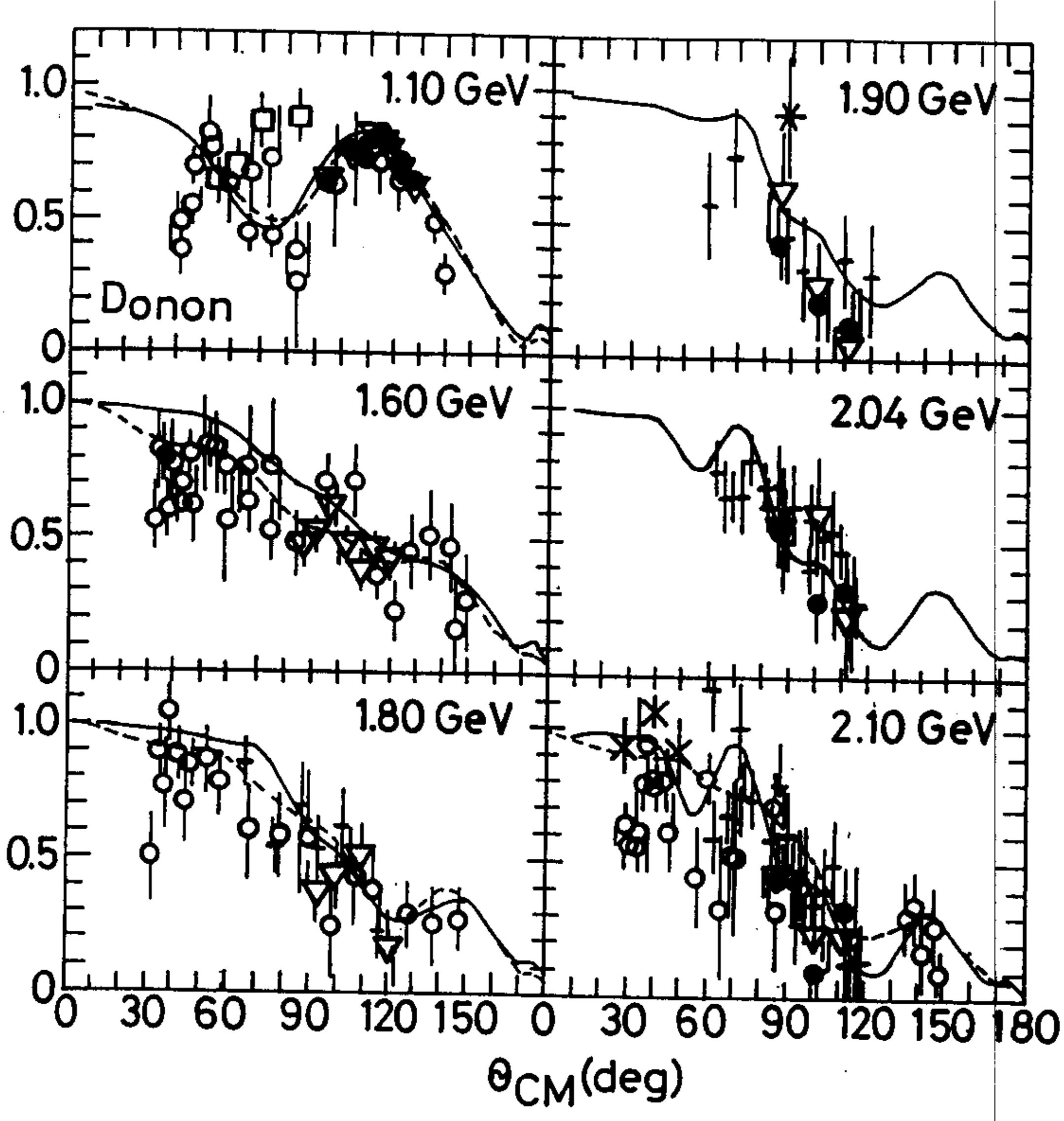
1.10 GeV
Donon
1.60 GeV
1.80 GeV
1.90 GeV
2.04 GeV
2.10 GeV
1.0
0.5
0
30
60
90
120
150
180
θCM(deg)

FIG. 9